

FORCED CONVECTION FLOW AND HEAT TRANSFER OF
NON-NEWTONIAN NANOFUIDS THROUGH A CIRCULAR TUBE

by

Gökhan Kıyak

B.S., Mechanical Engineering, Yıldız Technical University, 2014

Submitted to the Institute for Graduate Studies in
Science and Engineering in partial fulfillment of
the requirements for the degree of
Master of Science

Graduate Program in Mechanical Engineering
Boğaziçi University

2018

ACKNOWLEDGEMENTS

I would like to thank my thesis advisor Prof. Kunt Atalık for his valuable support during my studies. Studying under his supervision was a great experience for me. He helped me deepen my knowledge in engineering and taught how to ask the right questions through the solution journey.

Without my family support, it could not be possible to complete my studies and cope with obstacles that I have faced throughout my life. I am glad to have such a supportive family members who have always believed in me.

My friends Ömer Kocabey, Oğuz Akkuş, Doğukan Sakman, Çağlar Şahin and Sina Zare Pakzad are one of the most important part of this thesis. They have always motivated me to attain great successes.

ABSTRACT

FORCED CONVECTION FLOW AND HEAT TRANSFER OF NON-NEWTONIAN NANOFLUIDS THROUGH A CIRCULAR TUBE

Non-Newtonian nanofluids due to either non-Newtonian base fluid or high nanoparticle concentration flow cases have been numerically investigated through a circular tube under laminar flow condition. Governing equations have been solved in Fluent by utilizing Newtonian and non-Newtonian single-phase and two-phase models. Novel non-Newtonian two-phase modeling methods have been firstly applied in the current thesis. It can be said that two-phase modeling method with Granular model is better than two-phase model without solid phase viscosity from predictive power point of view because it requires less experiments on rheological characteristics. Heat transfer and pressure drop simulations have been compared with proposed correlations and experimental data in the literature. Heat transfer investigation results revealed that non-Newtonian Eulerian model without solid phase viscosity predicts the heat transfer coefficient better than the other single and two-phase models. Pressure drop simulation results show that non-Newtonian models are better than Newtonian models at pressure drop prediction of non-Newtonian nanofluids. Error rate decreases with increasing Reynolds number for all numerical modeling methods and single-phase non-Newtonian model gives the most accurate results. Finally, thermal performance of Newtonian and non-Newtonian nanofluids have been investigated in terms of convective heat transfer coefficient enhancement to pressure drop increment ratio. Thermal performance increases with increasing Reynolds number and decreasing nanoparticle concentration for both Newtonian and non-Newtonian nanofluids. It can be concluded that using a non-Newtonian nanofluid as a working fluid is more efficient than using a Newtonian nanofluid due to high pressure drop rate of Newtonian fluid flow.

ÖZET

NEWTONYEN OLMAYAN NANOAKIŞKANLARIN DAİRESEL BİR BORU BOYUNCA ZORLANMIŞ KONVEKSİYON AKIŞI VE ISI TRANSFERİ

Newtonyen olmayan baz akışkan ya da yüksek nanopartikül konsantrasyonu nedeni ile Newtonyen olmayan nanoakışkan durumları nümerik olarak laminer akış şartında dairesel bir boru boyunca incelenmiştir. Genel denklemler Newtonyen ve Newtonyen olmayan tek ve çift fazlı modeller kullanılarak Fluent'te çözülmüştür. Yeni Newtonyen olmayan iki fazlı modelleme metodları ilk olarak bu tezde uygulanmıştır. Granül modellenmiş iki fazlı modelleme metodunun öngörü gücü açısından katı faz viskozitesi olmayan iki fazlı modelden daha iyi olduğu söylenebilir, çünkü bu model reolojik özellikler üzerine daha az deney gerektirmektedir. Isı transferi ve basınç kaybı simülasyonları literatürdeki önerilen korelasyonlar ve deneysel veriler ile karşılaştırılmıştır. Isı transferi inceleme sonuçları, katı faz viskozitesi olmayan Newtonyen olmayan Eulerian modelin ısı transferi katsayısını diğer tek ve iki fazlı modellerden daha iyi tahmin ettiğini ortaya koymuştur. Basınç kaybı sonuçları ise Newtonyen olmayan modellerin Newtonyen olmayan nanoakışkanların basınç kaybı tahmininde Newtonyen modellerden daha iyi olduğunu göstermektedir. Tüm nümerik modelleme yöntemlerinde Reynolds sayısı arttıkça hata oranı azalmakta ve tek fazlı Newtonyen olmayan model en doğru sonuçları vermektedir. Son olarak, Newtonyen ve Newtonyen olmayan nanoakışkanların termal performansı basınç kaybı artışı ve ısı transferi artışlarının oranı açısından incelenmiştir. Termal performans, hem Newtonyen hem de Newtonyen olmayan nanoakışkanlarda Reynolds sayısı arttırıldığında ve nanopartikül konsantrasyonu azaltıldığında artmaktadır. Newtonyen olmayan bir nanoakışkanın çalışma sıvısı olarak kullanılması, Newtonyen akıştaki yüksek basınç kaybı oranı nedeniyle Newtonyen nanoakışkan kullanılmasından daha verimli olduğu sonucuna varılabilir.

TABLE OF CONTENTS

ACKNOWLEDGEMENTS	iii
ABSTRACT	iv
ÖZET	v
LIST OF FIGURES	vii
LIST OF TABLES	ix
LIST OF ACRONYMS/ABBREVIATIONS	xii
LIST OF SYMBOLS	xiii
1. INTRODUCTION	1
1.1. Literature Survey	1
1.2. Objective and Scope	6
2. MATHEMATICAL FORMULATION	7
2.1. Thermophysical Properties	7
2.2. Governing Equations	12
2.2.1. Single-Phase Model	12
2.2.2. Two-Phase Models	13
2.2.2.1. Eulerian Model	13
2.2.2.2. Mixture Model	14
3. NUMERICAL METHOD AND VALIDATION	17
3.1. Mesh Independency Tests for Water Flow	17
3.2. Validation for Newtonian Nanofluid Flow	20
3.3. Pressure Drop Simulations for Water Flow	22
4. RESULTS AND DISCUSSION	24
4.1. Heat Transfer Analysis	24
4.2. Pressure Drop Analysis	29
4.3. Thermal Performance Analysis	32
5. CONCLUSION	39
REFERENCES	42

LIST OF FIGURES

Figure 3.1.	Computational Domain.	17
Figure 3.2.	Mesh Views a)38511 Nodes b)73521 Nodes c)93031 Nodes d)117026 Nodes	18
Figure 3.3.	Mesh Independency Test for Water Flow at Re=1600 (D=10 mm, L=2.11 m).	19
Figure 3.4.	Mesh Independency Test for Water Flow at Re=1700 (D=3.97 mm, L=2 m).	20
Figure 3.5.	Local Nusselt Number Comparison for 1.6% Al_2O_3 -Water Nanofluid at Re=1600.	21
Figure 4.1.	Convective Heat Transfer Coefficient Comparison of Water Flow at Various Reynolds Number.	24
Figure 4.2.	Convective Heat Transfer Coefficient Comparison of 2.5% TNT- Water Flow at Re=1700.	28
Figure 4.3.	Heat Transfer Coefficient Increment Ratio of 0.5% CMC/Water Based Al_2O_3 Nanofluid to Base Fluid.	33
Figure 4.4.	Pressure Drop Increment Ratio of 0.5% CMC/Water Based Al_2O_3 Nanofluid to Base Fluid.	35
Figure 4.5.	Heat Transfer Coefficient Increment Ratio of Water Based Al_2O_3 Nanofluid to Base Fluid.	36

Figure 4.6. Pressure Drop Increment Ratio of Water Based Al_2O_3 Nanofluid to Base Fluid.	37
--	----

LIST OF TABLES

Table 2.1.	Power law (n) and consistency index (K) values for 0.5% <i>CMC</i> /water base fluid and Al_2O_3 nanofluid [1].	10
Table 2.2.	Base fluid and solid phase viscosities for 0.1% Al_2O_3 -0.5% <i>CMC</i> /water nanofluid.	10
Table 3.1.	Error rates (%) of local Nusselt number comparison for water by using various node numbers ($D=10$ mm, $L=2.11$ m).	20
Table 3.2.	Error rates (%) of local Nusselt number comparison for water by using various node numbers ($D=3.97$ mm and $L=2$ m).	21
Table 3.3.	Error rates (%) of single-phase and two-phase models for 1.6% Al_2O_3 -water nanofluid at $Re=1600$	22
Table 3.4.	Error rates (%) of pressure drop simulations at different Reynolds numbers.	23
Table 4.1.	Average convective heat transfer coefficient comparison for water flow.	25
Table 4.2.	Error rates (%) of Al_2O_3 -0.5% <i>CMC</i> /water experimental results and Newtonian single-phase and two-phase numerical models comparison.	26
Table 4.3.	Error rates (%) of Al_2O_3 -0.5% <i>CMC</i> /water experimental results and non-Newtonian single-phase and two-phase numerical models comparison.	27

Table 4.4.	Error rates (%) of 2.5% TNT-water flow (Newtonian/non-Newtonian single-phase and two-phase models comparison).	27
Table 4.5.	Error rates (%) of Newtonian Al_2O_3 -water nanofluid pressure drop simulation comparison with proposed correlation for non-Newtonian nanofluids (Equation 4.1).	30
Table 4.6.	Error rates (%) of Newtonian Al_2O_3 -water nanofluid pressure drop simulation comparison with the analytical correlation for Newtonian fluids (Equation 3.3).	31
Table 4.7.	Error rates (%) of non-Newtonian Al_2O_3 -0.5% CMC/water nanofluid pressure drop simulation comparison with the proposed correlation for non-Newtonian nanofluids (Equation 4.1).	32
Table 4.8.	Heat transfer coefficient increment rate (%) of 0.5% CMC/water based Al_2O_3 nanofluid.	34
Table 4.9.	Pressure drop increment rate (%) of 0.5% CMC/water based Al_2O_3 nanofluid compared to base fluid.	34
Table 4.10.	The ratio of convective heat transfer coefficient enhancement to pressure drop increase comparison of non-Newtonian Al_2O_3 -0.5% CMC/water nanofluid flow.	34
Table 4.11.	Heat transfer coefficient increment rate (%) of water based Al_2O_3 nanofluid compared to base fluid.	35
Table 4.12.	Pressure drop increment rate (%) of water based Al_2O_3 nanofluid compared to base fluid.	36

Table 4.13. The ratio of convective heat transfer coefficient enhancement to pressure drop increase comparison of Newtonian Al_2O_3 -water nanofluid flow.	38
--	----

LIST OF ACRONYMS/ABBREVIATIONS

CFD	Computational Fluid Dynamics
CMC	Carboxymethyl Cellulose
CNT	Carbon Nanotubes
GA	Gum Arabic
MWCNT	Multi-Walled Carbon Nanotubes
SP	Single-Phase
THW	Transient Hot-Wire
TP	Two-Phase

LIST OF SYMBOLS

\vec{a}	Acceleration vector
c_p	Specific heat
d_p	Nanoparticle diameter
f	Friction factor
h	Heat transfer coefficient
k	Thermal conductivity
n	Power law index
q''	Wall heat flux
D	Tube diameter
K	Consistency index
Nu	Nusselt number
P	Pressure
Pe	Peclet number
Pr	Prandtl number
Re	Reynolds number
T	Temperature
\vec{V}	Velocity vector
X	Axial distance from inlet
$\dot{\gamma}$	Shear rate
η	Non-Newtonian viscosity
μ	Viscosity
ρ	Density
ϕ	Nanoparticle volume concentration

1. INTRODUCTION

1.1. Literature Survey

Heat transfer rate can be increased by increasing heat transfer coefficient or increasing heat transfer surface area. Increasing heat transfer surface will lead bigger size of heat exchanger which requires more space and contradicts need for smaller size heat exchangers. Scientists who have these concerns have tried to increase thermal conductivity of conventional liquids by adding nanosized solid particles with higher thermal conductivities. Pioneering works have been done by Maxwell [2] and Masuda *et al.* [3] on this subject. After Choi and Eastman's study [4], these solutions have been named as nanofluids.

Nanofluids are prepared by using two main approaches. These are one-step method and two-step method. One-step method indicates that preparation of nanofluid is completed in one step and additional steps are not needed. For instance, nanoparticles and the base fluid chemically react with each other and nanofluid is produced as a result of this reaction. Two-step method is the other preparation method of nanofluids which is widely used because of its applicability to various base fluid and nanoparticle combinations. This method is applied by directly mixing the nanoparticle and the base fluid. However, nanoparticle aggregation is observed after a while and additional steps are required. To obtain a stable nanoparticle and base fluid solution, researchers apply ultrasonication or add surfactants such as Gum Arabic (GA) or Carboxymethyl Cellulose (CMC) [5].

To evaluate the flow behavior and heat transfer effects of nanofluids, thermophysical properties have to be known. Kakaç and Pramuanjaroenkij's review paper [6] shows that many researchers have experimentally measured thermal conductivity and viscosity of nanofluids. Instead of conducting experiments for every single nanofluid, many correlations have been proposed to evaluate thermophysical properties such as thermal conductivity and viscosity based on experimental data [6, 7]. These correla-

tions differ from each other in terms of including nanoparticle concentration, diameter and shape effects, temperature dependency, Brownian motion effect, etc. For example, thermal conductivity model of Hamilton and Crosser [8] includes shape and nanoparticle concentration effects. Heyhat *et al.*'s model [9] shows temperature and nanoparticle concentration effects on thermal conductivity and Chon *et al.*'s model [10] considers the Brownian motion. Lastly, Kamali and Binesh [11] obtained a temperature dependent correlation by curve-fitting the experimental results. Additionally, Newtonian viscosity of nanofluids have been described by many correlations. Maiga *et al.* [12] and Heyhat *et al.* [9] introduced nanoparticle concentration and temperature dependent viscosity models, respectively. Many other correlations have been proposed for different nanoparticle-nanofluid combination and nanoparticle concentration cases. They can be found in the literature.

After evaluating thermophysical properties of nanofluids, researchers have focused on flow behaviors of Newtonian and non-Newtonian nanofluids. In scope of Newtonian nanofluid flow, Suresh *et al.* [13], Wen and Ding [14], Akhavan-Zanjani *et al.* [15], Yang *et al.* [16], Cabaleiro *et al.* [17], Pourfayaz *et al.* [18], İlhan and Ertürk [19] and Noghrehabadi *et al.* [20] experimentally studied forced convection of nanofluids under laminar flow and constant heat flux boundary condition. Their experiments on various combination of base fluids and nanoparticles reveal that thermal conductivity and viscosity values increase as nanoparticle concentration increases. Additionally, heat transfer coefficient and pressure drop raise with increasing Reynolds number and nanoparticle concentration.

Furthermore, many scientists have numerically studied Newtonian nanofluid flow. To mention a few, Utomo *et al.* [21], Maiga *et al.* [12, 22], Purohit *et al.* [23], Colla *et al.* [24] and Elahmer *et al.* [25] have used single-phase model to investigate convective heat transfer increment of nanofluids. Purohit *et al.*'s [23] single-phase numerical model showed that nanofluid's performance factor decreases with increasing nanoparticle concentration. Ho *et al.* [26] also experimentally and numerically studied forced convection and pressure drop of Newtonian Al_2O_3 /water flow under laminar flow range. Their study showed heat transfer and pressure drop increment with ad-

dition of nanoparticles and more accurate numerical results with using temperature dependent properties. Usage of two-phase modeling methods can be seen at numerical studies of Goktepe *et al.* [27], Moghadassi *et al.* [28], Ambreen and Kim [29], Sekrani and Poncet [30] and Behroyan *et al.* [31] on laminar forced convection of nanofluids. Their results reveal increment of heat transfer coefficient and pressure drop by adding nanoparticles. Additionally, it can be seen from their studies that two-phase models give more accurate results compared to single-phase models.

Newtonian behavior of base fluids can be converted to non-Newtonian due to nanoparticle loading [32]. High concentration causes aggregation of nanoparticles, change in cluster structure and internal shear stress. In this case, Newtonian viscosity models cannot describe the rheological behavior of the fluid. Thus, non-Newtonian viscosity models have been proposed such as power law, Carreau-Bird, Cross viscosity, Bingham plastic, Herchel-Bulkey and Casson [33]. Thermal conductivity models are used as they are in the Newtonian nanofluid case.

Phuoc and Massoudi [34] examined rheological behavior of Fe_2O_3 /deionized water nanofluids. They observed shear-thinning non-Newtonian viscosity after exceeding 0.02 nanoparticle volume fraction. Kole and Dey's [35] CuO /gear oil nanofluid showed non-Newtonian behavior after 0.5 volume% nanoparticle loading. Minakov *et al.* [36] experimentally studied water based CuO nanofluid flow under constant wall heat flux boundary condition. Their study showed that Newtonian behavior of the nanofluid became non-Newtonian after 0.25% CuO nanoparticle loading. Heat transfer increment has been observed with increasing nanoparticle concentration. For 2% CuO nanofluid flow and fixed Reynolds number, heat transfer coefficient is almost doubled compared to base fluid. Chen *et al.* [37] conducted experiments on laminar convection of water based titanate nanotubes. Their shear thinning non-Newtonian nanofluid suspension exhibits higher convective heat transfer coefficient enhancement than thermal conductivity increment. They also observed that heat transfer coefficient increases with increasing Reynolds number, reaches its maximum at the inlet region and decreases with increasing axial distance. Paul *et al.*'s experiments [38] on Al_2O_3 added ionic water showed that nanoparticle addition changes fluid's rheological behavior from Newtonian

to non-Newtonian. They investigated heat transfer properties of the nanofluid through a circular pipe under constant heat flux boundary condition. They concluded their study with stating heat transfer increment with increasing nanoparticle concentration and Reynolds number.

Numerical studies have also carried out to study non-Newtonian fluids due to high nanoparticle concentration. Single-phase non-Newtonian model is mostly used for simulating this kind of nanofluids. After conducting experiments, Minakov *et al.* [39] numerically examined *CuO*/water nanofluids with up to 2 volume% by utilizing power law model. Their numerical model gave satisfactory results compared to experimental study. They claim that deviations between numerical results and experimental results might be caused by incorrect thermophysical correlations. Furthermore, He *et al.* [40] numerically studied on forced convective heat transfer of non-Newtonian nanofluids by comparing Newtonian and non-Newtonian viscosity models. Their results for 2.5 weight% *TNT*/water case showed that there was not a significant difference between using Newtonian or non-Newtonian model because they gave similar error rates compared to experimental results.

Nanofluids can also have their non-Newtonian characteristics by non-Newtonian nature of base fluids or addition of surfactants to stabilization. Hojjat *et al.* [41–43] prepared 0.5 volume% carboxymethyl cellulose (*CMC*)/water based nanofluids to examine their heat transfer and pressure drop properties. Their forced convection analysis under constant wall temperature and constant heat flux boundary condition revealed that nanoparticle addition into the non-Newtonian base fluid significantly increases the convective heat transfer coefficient. Additionally, their pressure drop experiments showed that there is not a drastic increase in pressure loss with addition of nanoparticles. They concluded their study with proposing a correlation to predict pressure drop of non-Newtonian nanofluids in laminar and turbulent flow regime. Garg *et al.* [44] also experimentally studied 0.25 weight% Gum Arabic (*GA*)/water based multi-walled carbon nanotubes (*MWCNT*) added nanofluids. They observed 32% heat transfer increment at around $Re=600$ which was higher than maximum 20% thermal conductivity increase. Ding *et al.* [45] conducted experiments on heat transfer of carbon

nanotubes (*CNT*) added nanofluids. Their base fluid was non-Newtonian 0.25 weight% *GA/water*. They observed heat transfer increase with reaching its maximum at the entrance region. Mahrood *et al.* [46] experimentally studied natural convection of $Al_2O_3 - CMC$ and $TiO_2 - CMC$ nanofluids. Their experiments showed that there is an optimum point of nanoparticle loading. 0.2% and 0.1% concentrations were found to be the best nanoparticle loadings for $Al_2O_3 - CMC$ and $TiO_2 - CMC$ nanofluids, respectively. Increasing nanoparticle concentration worsened heat transfer performance of their non-Newtonian nanofluids. Javadpour's *et al.* [47] experimental study on 0.2 weight% *CMC/water* based *CuO* nanofluid with up to 1.5% nanoparticle concentration showed that lowered thermal boundary layer thickness, raised thermal entry length caused by shear-thinning viscosity and enhanced thermal conductivity are main causes of increased heat transfer coefficient. Their study also revealed highest average heat transfer increment of 25.3% for 1.5% nanoparticle concentration at $Re=1280$.

Non-Newtonian based nanofluids have been numerically investigated by many researchers. Computational fluid dynamics (CFD) has been used for forced convection of Al_2O_3 and Xanthan aqueous solution by Moraveji *et al.* [48]. Single-phase non-Newtonian modeling method has been used in their study through a circular pipe under constant wall heat flux boundary condition. Rheological behavior was described by Herschel–Bulkley model. Their results reveal that convective heat transfer increases with increasing nanoparticle concentration and Reynolds number. They also observed that increasing particle diameter and decreasing concentration of Xanthan aqueous solution had positive effect on heat transfer. Moreover, Kamali and Binesh [11] numerically investigated heat transfer increment of non-Newtonian *MWCNT* nanofluids through a tube under constant heat flux condition. They used single-phase non-Newtonian modeling method and power law model to describe non-Newtonian viscosity. Thermal conductivity of nanofluids was explained by third degree polynomial equation in their study. Forced convection simulation results at different Reynolds number in laminar flow case revealed that their numerical study is in good agreement with experimental data. He *et al.* [40] also numerically studied forced convection 0.25 weight% *GA/water* based *CNT* nanofluids through a circular pipe under laminar flow condition. Their results reveal that non-Newtonian single-phase model shows better agreement with

experimental results than that of Newtonian single-phase model. Labib *et al.* [49] simulated forced convection of non-Newtonian based Al_2O_3 added nanofluid by using mixture model. They utilized non-Newtonian 0.1% CNT-water nanofluid as a base fluid and combined it with Al_2O_3 nanoparticles. They observed significant increase in the heat transfer coefficient due to lowered thermal boundary layer thickness caused by shear thinning base fluid.

1.2. Objective and Scope

In scope of the current study, forced convection and pressure drop of non-Newtonian nanofluids will be numerically investigated under laminar flow condition. Due to lack of non-Newtonian two-phase model simulations, novel non-Newtonian two-phase modeling methods are proposed and utilized in this thesis. Comparison of proposed models and classical single-phase and two-phase models have been done on experimental studies. First of all, heat transfer comparisons have been conducted on experimental studies of Hojjat *et al.* [41] and Chen *et al.* [37]. Secondly, pressure drop simulation results have been checked against a proposed correlation by Hojjat *et al.* [42] in their experimental study on pressure drop of non-Newtonian nanofluids. Finally, thermal performance of Newtonian and non-Newtonian nanofluids has been evaluated in terms of convective heat transfer and pressure drop increment ratio.

To this end, literature survey has been compiled in the introduction chapter and numerical details behind the simulations have been given in the following mathematical formulation chapter. Mesh independency tests have been done and numerical simulation accuracy has been checked in the chapter 3. Additionally, proposed models and existing models have been compared with experimental studies in the results and discussion chapter. Conclusion has been summarized in the last chapter.

2. MATHEMATICAL FORMULATION

2.1. Thermophysical Properties

Thermophysical properties can be measured experimentally. However, it is expensive and time-consuming. To overcome these obstacles, researchers have been proposed many correlations to calculate effective thermophysical properties of nanofluids.

Density of nanoparticle and base fluid mixture can be calculated as follows [22],

$$\rho_{nf} = (1 - \phi_p)\rho_{bf} + \phi_p\rho_p \quad (2.1)$$

where ρ_{nf} , ρ_{bf} , ρ_p are nanofluid density, base fluid density, nanoparticle density and ϕ_p nanoparticle volume concentration, respectively.

To calculate specific heat of nanofluids, below classical model can be used [50],

$$\rho_{nf}c_{p,nf} = (1 - \phi_p)\rho_{bf}c_{p,bf} + \phi_p\rho_p c_{p,p} \quad (2.2)$$

where $c_{p,nf}$, $c_{p,bf}$, $c_{p,p}$ are nanofluid specific heat, base fluid specific heat and nanoparticle specific heat, respectively.

Effective thermal conductivity of the nanofluid has been calculated according to Chon *et al.*'s [10] proposed model which includes the Brownian motion effect, temperature dependency, nanoparticle diameter and concentration dependency. Below correlation can be used for 11 to 150 nm nanoparticle diameter and 21 to 71 °C temperature

range [10].

$$k_{nf} = k_{bf} \left(1 + 64.7(\phi_p^{0.764}) \left(\frac{d_{bf}}{d_p} \right)^{0.369} \left(\frac{k_{bf}}{k_p} \right)^{0.7476} Pr^{0.9955} Re_{np}^{1.2321} \right) \quad (2.3)$$

where k_{nf} , k_{bf} , k_p are nanofluid thermal conductivity, base fluid thermal conductivity and nanoparticle thermal conductivity, respectively. Additionally, nanoparticle Reynolds number equals to;

$$Re_{np} = \frac{\rho_{bf} K_B T}{3\pi \mu_{bf}^2 \lambda} \quad (2.4)$$

where $\lambda = 0.17$ nm is the mean free path for water and $K_B = 1.3807 \times 10^{-23}$ J/K is the Boltzmann constant.

Based on nanoparticle concentration and base fluid viscosity, Pak and Cho [51] have proposed a model to calculate viscosity of nanofluids. Effective viscosity of Newtonian nanofluids,

$$\mu_{nf} = (1 + 39.11\phi_p + 533.9\phi_p^2)\mu_{bf} \quad (2.5)$$

where μ_{nf} , μ_{bf} are nanofluid viscosity and base fluid viscosity, respectively. Base fluid viscosity is described as,

$$\mu_{bf} = A10^{\left(\frac{B}{T-C}\right)} \quad (2.6)$$

where $A = 2.414 \times 10^{-5}$, $B = 247.8$, $C = 140$.

Effective viscosity calculation method can vary for the two-phase models. Two different two-phase viscosity modeling methods have been applied in scope of this study. The value obtained by Equation 2.5 has been utilized as a reference value for the single-phase and two-phase 1 (TP1) cases. For the two-phase 2 (TP2) case, base fluid has its own viscosity (Equation 2.6) and solid phase viscosity is determined by Miller and Gidaspow equation [52]. Which is given as,

$$\mu_p = -0.188 + 537.4\phi_p \quad (2.7)$$

For a non-Newtonian fluid that can be expressed by the power law model, the apparent viscosity is described as,

$$\eta = K\dot{\gamma}^{n-1} \quad (2.8)$$

where K is the consistency index and n is the power law index. Unless otherwise stated, K and n values are obtained from Hojjat *et al.*'s experimental study [1] on rheological characteristics of non-Newtonian nanofluids.

In the two-phase non-Newtonian cases, viscosity of nanoparticle and base fluid have been determined according to below two cases. In the first case (TP1), non-Newtonian viscosity of nanofluid is assigned to the base fluid and nanoparticle viscosity is chosen zero. In the second case (TP2), base fluid has its own non-Newtonian viscosity. Nanoparticle viscosity is determined by Miller and Gidaspow equation (Equation 2.7) [52].

To illustrate how viscosities are chosen for the base fluid and the solid phase, below tables have been prepared. Power law index and consistency index for the base fluid (0.5% CMC/water) and 0.1% Al_2O_3 nanofluid can be seen in Table 2.1.

Table 2.1. Power law (n) and consistency index (K) values for 0.5% *CMC*/water base fluid and Al_2O_3 nanofluid [1].

	n	K
Base fluid	0.5739	0.1005
0.1% Al_2O_3	0.5417	0.1241
0.2% Al_2O_3	0.5417	0.1537
0.5% Al_2O_3	0.5154	0.1655
1.0% Al_2O_3	0.5534	0.1271
1.5% Al_2O_3	0.5202	0.1685

Table 2.2. Base fluid and solid phase viscosities for 0.1% Al_2O_3 -0.5% *CMC*/water nanofluid.

Model	Base fluid		Solid phase
TP1	Equation 2.8	n=0.5417	-
		K=0.1241	
TP2	Equation 2.8	n=0.5739	Equation 2.7
		K=0.1005	

Base fluid and solid phase viscosities for 0.1% Al_2O_3 nanofluid according to TP1 and TP2 modeling methods can be seen in Table 2.2.

Dimensionless Nusselt, Prandtl, Reynolds and Peclet numbers can be described as,

Nusselt number is basically defined as the ratio of convection to conduction.

$$Nu = \frac{hD}{k} \quad (2.9)$$

where h is the convective heat transfer coefficient and D is the tube diameter.

Prandtl number is the ratio of momentum diffusion to thermal diffusion.

$$Pr = \frac{c_p K \left(\frac{V}{D}\right)^{n-1}}{k} \quad (2.10)$$

Reynolds number is the ratio of inertial force to viscous force. For a Newtonian fluid, it can be described as,

$$Re = \frac{\rho V D}{\mu} \quad (2.11)$$

Reynolds number definition is changed for non-Newtonian fluids. For a non-Newtonian fluid, it can be expressed as,

$$Re = \frac{\rho V^{2-n} D^n}{K} \quad (2.12)$$

Peclet number can be obtained by multiplying Prandtl and Reynolds numbers. It expresses the ratio of energy conducted to the fluid to energy conducted within the fluid.

$$Pe = \frac{\rho c_p V D}{k} \quad (2.13)$$

2.2. Governing Equations

2.2.1. Single-Phase Model

In the single-phase model consideration, nano-sized solid particles and base fluid are thought to be thermally and hydrodynamically in equilibrium and slip velocity between the phases is zero. These phases are treated as one single homogeneous fluid with having shared effective thermophysical properties [53]. Examples of theoretical models to calculate effective properties can be seen in the aforementioned equations.

For a steady state conventional fluid, governing equations can be described as,

Continuity,

$$\nabla \cdot (\rho_{nf} \vec{V}) = 0 \quad (2.14)$$

where \vec{V} is the velocity vector.

Momentum conservation,

$$\nabla \cdot (\rho_{nf} \vec{V} \vec{V}) = -\nabla P + \mu_{nf} \nabla^2 \vec{V} \quad (2.15)$$

where P is the pressure.

Energy conservation,

$$\nabla \cdot (\rho_{nf} c_{p,nf} \vec{V} T) = \nabla \cdot (k_{nf} \nabla T) \quad (2.16)$$

where T is the temperature.

2.2.2. Two-Phase Models

Newtonian and non-Newtonian Eulerian and mixture model will be applied in scope of this study.

2.2.2.1. Eulerian Model. Continuity equation, momentum equation and energy equation are solved separately for each phase in the Eulerian model consideration even if solid and liquid phases share one single pressure. Velocity and temperature differences are taken into account and governing equations are solved by using the finite volume method [7].

Mass conservation is described as,

$$\nabla \cdot (\phi_q \rho_q \vec{V}_q) = 0 \quad (2.17)$$

where $\vec{V}_q = \int_V \phi_q dV$, $\sum_{q=1}^n \phi_q = 1$ and q shows the phases.

Momentum conservation can be stated as,

$$\nabla \cdot (\phi_q \rho_q \vec{V}_q \vec{V}_q) = -\phi_q \nabla P + \phi_q \mu_q \nabla^2 \vec{V} + \sum_{p=1}^n \vec{R}_{pq} \quad (2.18)$$

where $\sum_{p=1}^n \vec{R}_{pq} = \sum_p S_{pq} (\vec{V}_p - \vec{V}_q)$ is the interaction drag forces from base fluid phase to nanoparticle phase, $S_{pq} = (\phi_q \phi_p \rho_q f) / \tau_p$, $\tau_p = (\rho_p d_p^2) / (18\mu^2)$ and f expresses the drag friction. It is found according to Schiller [54] as,

$$f = \frac{C_D Re_p}{24} \quad (2.19)$$

$$C_D = \begin{cases} \frac{24(1+0.15Re_p^{0.687})}{Re_p}, & Re_p \leq 1000 \\ 0.44, & Re_p > 1000 \end{cases} \quad (2.20)$$

$$Re_p = \frac{\rho_q |\vec{V}_p - \vec{V}_q| d_p}{\mu_q} \quad (2.21)$$

Energy conservation,

$$\nabla \cdot (\phi_q \rho_q c_{p,q} \vec{V}_q T_q) = \nabla \cdot (\phi_q k_{eff,q} \nabla T_q) + \sum_{p=1}^n Q_{pq} \quad (2.22)$$

where $Q_{pq} = h(T_p - T_q)$ and the heat transfer coefficient is $h = \frac{6k_d \phi_q \phi_p Nu_p}{d_p^2}$. Nu_p is evaluated from the Ranz *et al.*'s proposed model [55],

$$Nu_p = 2 + 0.6Re_p^{0.5} Pr_q^{0.333} \quad (2.23)$$

where $Pr_q = (c_{p,q} \mu_q) / k_d$.

2.2.2.2. Mixture Model. Mixture model assumes one single fluid which has two separate phases. These phases have their own velocity and volume concentration. Continuity, momentum and energy equations are not solved separately, but they are solved for the mixture [7].

The mass conservation equation is written as,

$$\nabla \cdot (\rho_m \vec{V}_m) = 0 \quad (2.24)$$

where \vec{V}_m is the mass average velocity and described as,

$$\vec{V}_m = \frac{\sum_{k=1}^n \phi_k \rho_k \vec{V}_k}{\rho_m} \quad (2.25)$$

The momentum conservation is obtained as,

$$\nabla \cdot (\rho_m \vec{V}_m \vec{V}_m) = -\nabla P_m + \mu_m \nabla^2 \vec{V} + \nabla \cdot \left(\sum_{k=1}^n \phi_k \rho_k \vec{V}_{dr,k} \vec{V}_{dr,k} \right) \quad (2.26)$$

where $\vec{V}_{dr,k}$ is the drift velocity of the k^{th} phase and expressed as,

$$\vec{V}_{dr,k} = \vec{V}_k - \vec{V}_m \quad (2.27)$$

The relative (slip) velocity is described as the velocity of secondary phase (p) relative to the velocity of the primary phase (f) and given with the below equation.

$$\vec{V}_{pf} = \vec{V}_p - \vec{V}_f \quad (2.28)$$

The relation between drift velocity and relative velocity is,

$$\vec{V}_{dr,p} = \vec{V}_{pf} - \sum_{k=1}^n \frac{\phi_k \rho_k}{\rho_m} \vec{V}_{fk} \quad (2.29)$$

Manninen *et al.* [56] have proposed a correlation to find the relative velocity,

$$\vec{V}_{pf} = \frac{\tau_p d_p^2}{18 \mu_f f_{drag}} \frac{(\rho_p - \rho_m)}{\rho_p} \vec{a} \quad (2.30)$$

The acceleration vector ' \vec{a} ' is found as,

$$\vec{a} = \vec{g} - (\vec{V}_m \cdot \nabla) \vec{V}_m \quad (2.31)$$

Volume fraction of secondary phase,

$$\nabla \cdot (\phi_p \rho_p \vec{V}_m) = - \nabla \cdot (\phi_p \rho_p \vec{V}_{dr,p}) \quad (2.32)$$

Energy conservation is written as,

$$\nabla \cdot \left(\sum_{k=1}^n \rho_k \phi_k c_{p,k} T_k \vec{V}_k \right) = \nabla \cdot (k_{eff} \nabla T) \quad (2.33)$$

Mathematical formulations behind the numerical simulations have been summarized in the current chapter. Single-phase and two-phase models (Eulerian and mixture) will be used by applying Newtonian and non-Newtonian viscosity models.

3. NUMERICAL METHOD AND VALIDATION

3.1. Mesh Independency Tests for Water Flow

The numerical methods accessible in the CFD simulation software of Ansys Fluent have been used for the current study. Fluent uses a finite volume technique to transform the governing partial differential equations into a system of discrete algebraic equations. As discretization methods, a second-order upwind scheme is preferred for the momentum and energy solutions. All these conditions are the same for solving governing equations of both single and two-phase models. Thermophysical properties of the fluid, inlet velocity, inlet temperature and wall heat flux are given as the input parameters.

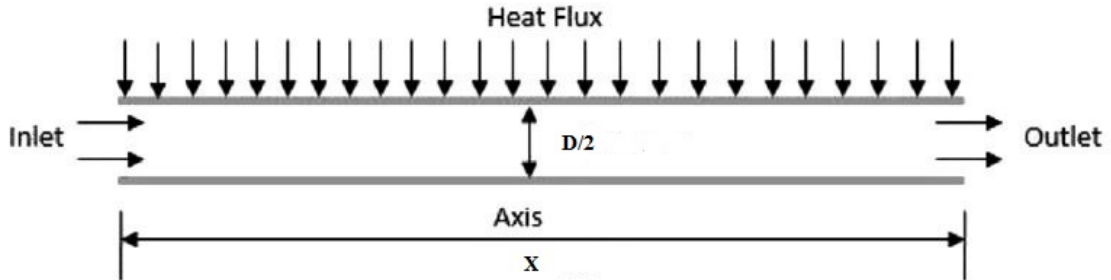


Figure 3.1. Computational Domain.

Due to axisymmetry and computational cost reduction, one-half of the test section will be simulated by using a 2 dimensional computational domain. Figure 3.1 shows computational domain and boundary conditions. Constant heat flux and no-slip boundary condition will be applied through the tube wall and zero gauge pressure is assumed at the tube outlet. The flow is thought to be thermally developing, hydrodynamically fully developed, steady, incompressible and laminar internal flow.

After proving mesh independency, current numerical models will be checked against well-known empirical equations in scope of validation. In the results and discussion session, two experimental studies which have different geometries will be simulated. Thus, mesh independency tests will be conducted for two pipe geometries.

Firstly, water flow through a circular pipe which has 2.11 m length and 10 mm inner diameter case has been simulated. 1500 W/m^2 constant heat flux has been applied through the pipe wall.

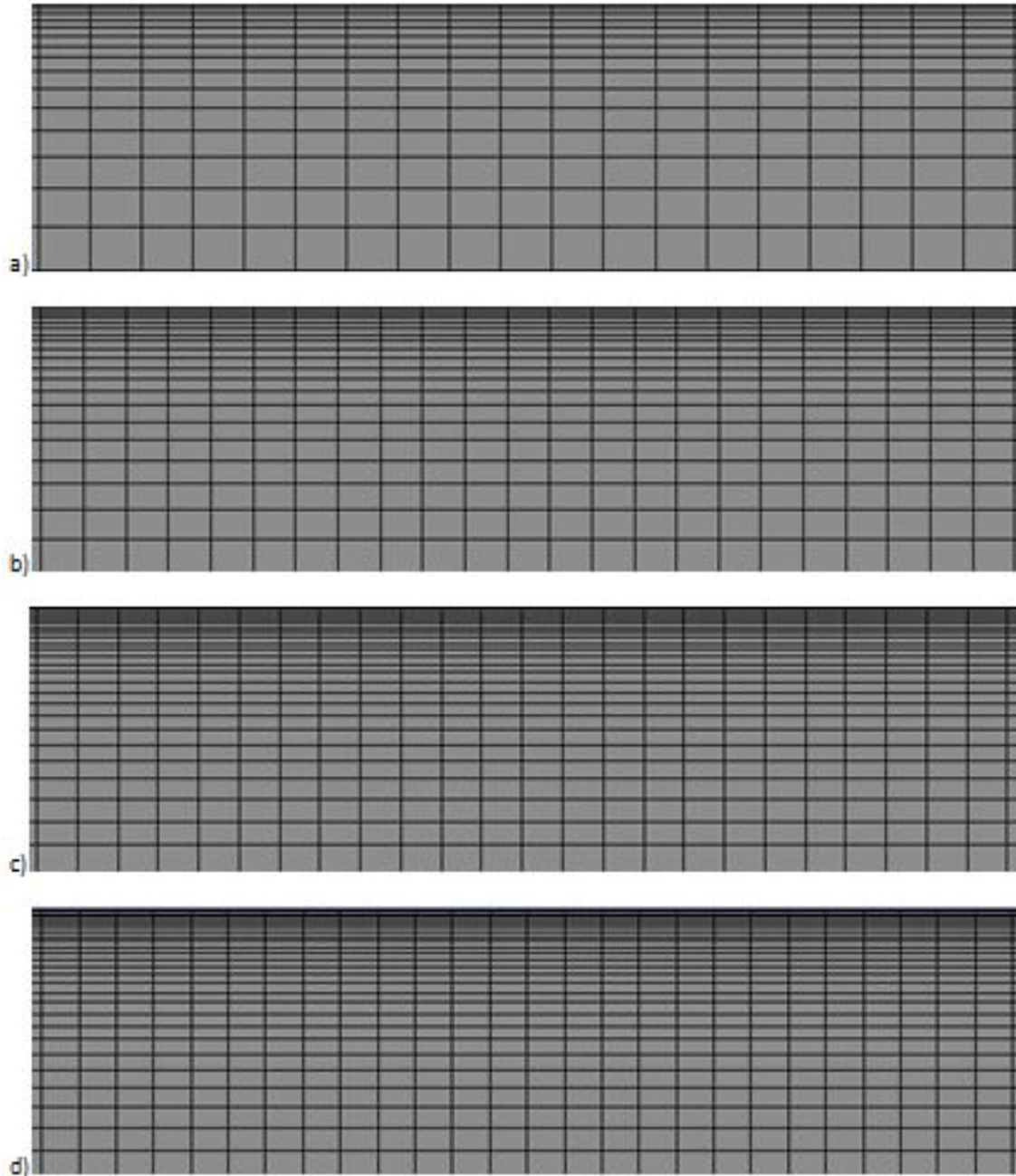


Figure 3.2. Mesh Views a)38511 Nodes b)73521 Nodes c)93031 Nodes d)117026 Nodes

By using various node sizes, water flow case simulations have been done. Figure 3.2 illustrates the mesh views. Finer grid is attained at the near vicinity of the tube wall because of more dominant inconsistencies at this area. Water flow cases have been

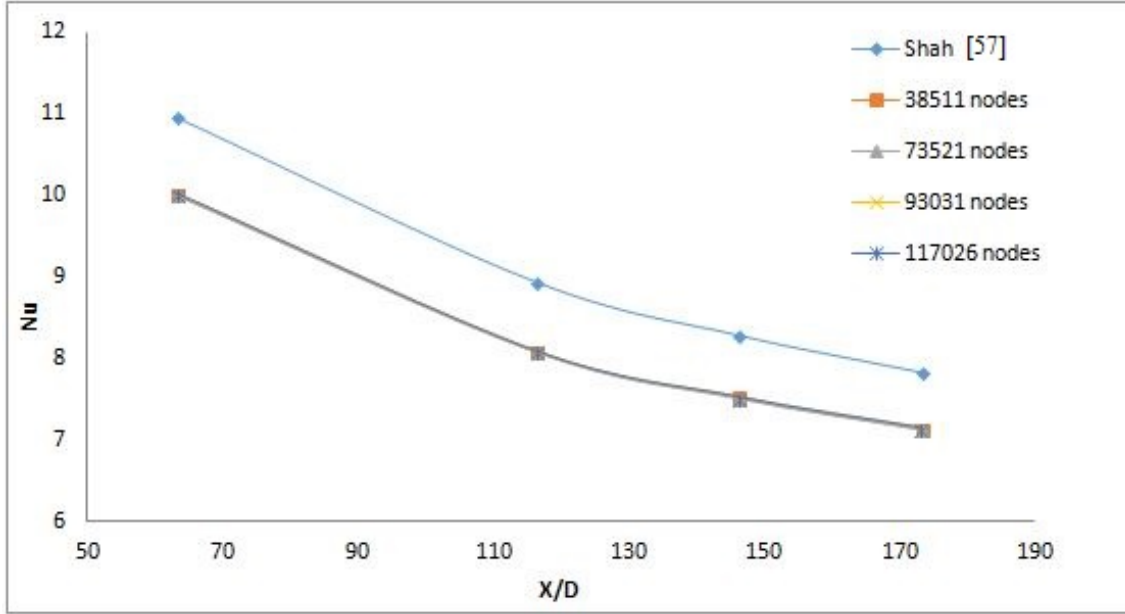


Figure 3.3. Mesh Independence Test for Water Flow at $Re=1600$ ($D=10$ mm, $L=2.11$ m).

compared with Shah equation [57]. Shah equation [57] is described as,

$$Nu = \begin{cases} 1.953 \left(Re Pr \frac{D}{X} \right)^{1/3} & \left(Re Pr \frac{D}{X} \right) \geq 33.3 \\ 4.364 + 0.0722 Re Pr \frac{D}{X} & \left(Re Pr \frac{D}{X} \right) < 33.3 \end{cases} \quad (3.1)$$

Simulation results can be seen in Figure 3.3 and Table 3.1. Error rate of numerical single-phase water flow results converges to 9.05% average error rate compared to Shah equation [57]. 93031 node number is the best mesh size for this case.

Current single-phase Newtonian model shows good agreement with Shah equation [57] in terms of water flow simulation. Deviation from the correlation decreases as node number increases.

Additionally, another mesh independency test has been done for a pipe which has 2 m length and 3.97 mm diameter. 1500 W/m^2 constant heat flux has been applied and tests have been conducted at $Re=1700$. Results can be seen in Figure 3.4 and Table 3.2.

Table 3.1. Error rates (%) of local Nusselt number comparison for water by using various node numbers (D=10 mm, L=2.11 m).

X/D	38511 nodes	73521 nodes	93031 nodes	117026 nodes
63	8.81	8.72	8.63	8.63
116	9.67	9.56	9.56	9.56
146	9.35	9.35	9.23	9.23
173	9.05	8.92	8.79	8.79
Average Error (%)	9.22	9.14	9.05	9.05

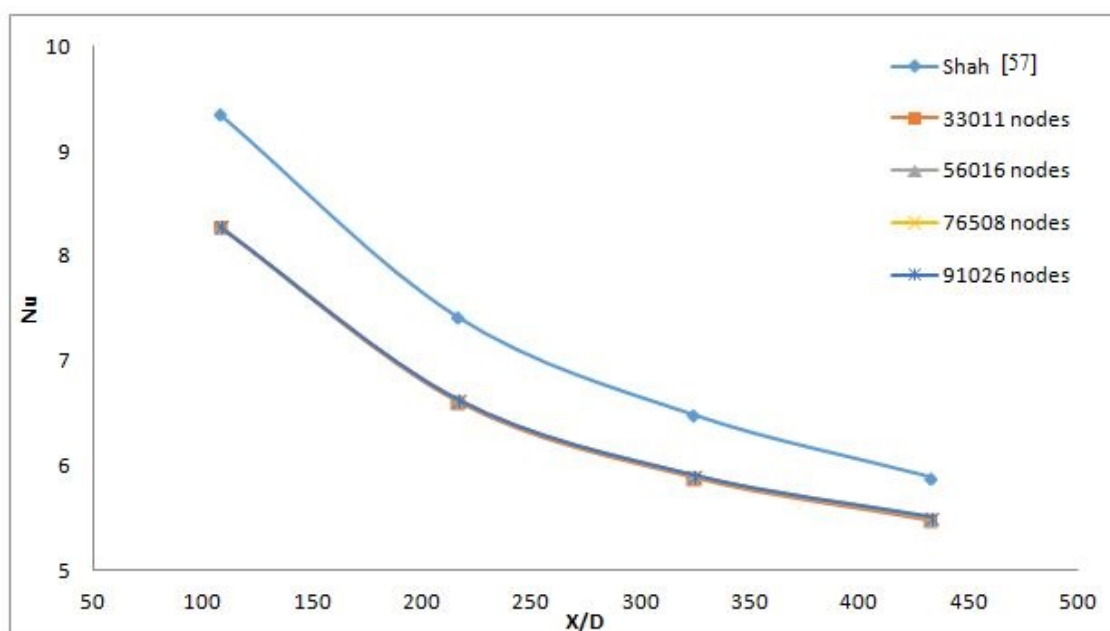


Figure 3.4. Mesh Independency Test for Water Flow at Re=1700 (D=3.97 mm, L=2 m).

Table 3.2 shows that average error rate converges to 9.34%. 76508 node size is chosen for this geometry.

3.2. Validation for Newtonian Nanofluid Flow

In scope of numerical model validation, 1.6% Al_2O_3 /water nanofluid flow cases have been studied by using Newtonian/ non-Newtonian single-phase models and mixture, and Eulerian two-phase models. Geometry of simulation domain consists of 2.11 m length and 10 mm diameter. For this geometry, 93031 node size is applied as it is

Table 3.2. Error rates (%) of local Nusselt number comparison for water by using various node numbers (D=3.97 mm and L=2 m).

X/D	33011 nodes	56016 nodes	76508 nodes	91026 nodes
108	11.49	11.42	11.39	11.39
216	10.84	10.61	10.58	10.58
324	9.20	8.90	8.89	8.89
432	7.02	6.68	6.51	6.51
Average Error (%)	9.64	9.40	9.34	9.34

stated at mesh independency tests.

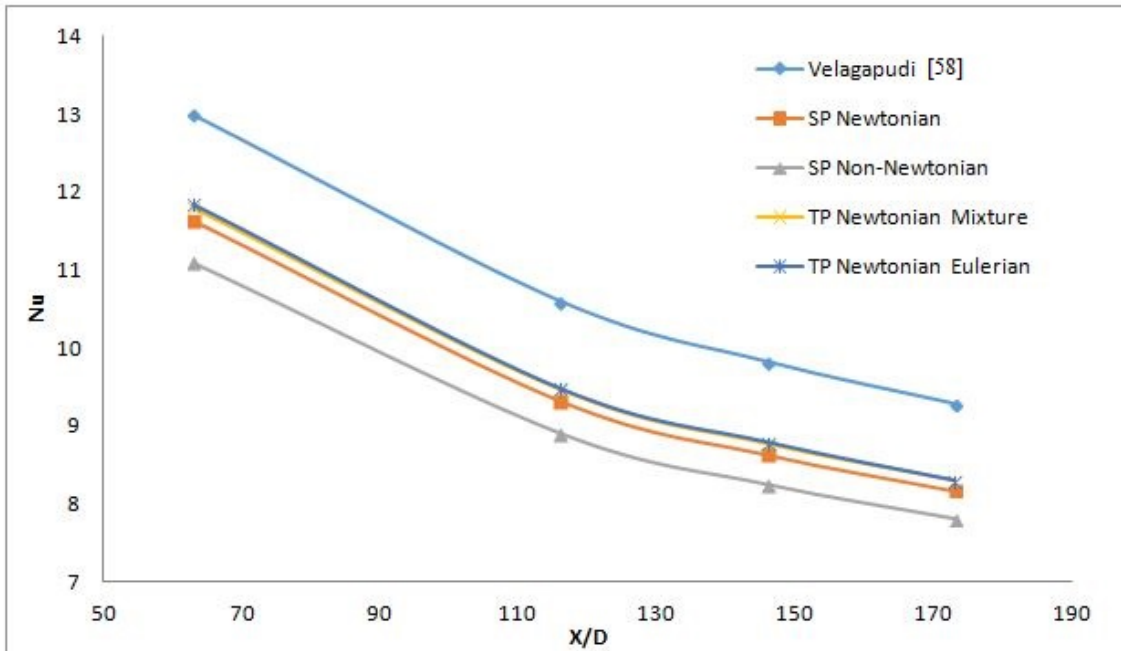


Figure 3.5. Local Nusselt Number Comparison for 1.6% Al_2O_3 -Water Nanofluid at $Re=1600$.

Velagapudi *et al.*'s correlation [58] comparison with the current numerical study can be seen in Figure 3.5 and Table 3.3 for 1.6% Al_2O_3 /water. Results show that current numerical study has minimum average error rate of 7.94%. Velagapudi *et al.*'s correlation [58] is,

$$Nu_{nf} = 1.98 \left(Re_{nf} Pr_{nf} \frac{D}{X} \right)^{0.333} \quad (3.2)$$

Table 3.3. Error rates (%) of single-phase and two-phase models for 1.6% Al_2O_3 -water nanofluid at Re=1600.

X/D	SP Newt.	SP Non-Newt.	TP Mixture	TP Eulerian
63	10.55	14.55	9.24	6.40
116	12.08	15.94	10.75	8.32
146	12.12	15.99	10.79	8.44
173	11.96	15.84	10.67	8.59
Average Error (%)	11.68	15.58	10.36	7.94

Results revealed that two-phase Newtonian models are in good agreement with Velagapudi equation [58]. Mixture and Eulerian models gave 10.36% and 7.94% average error rate compared to Velagapudi *et al.*'s equation [58]. According to simulation results, Eulerian model gives the least error rate.

Consistency index and power law index values for single-phase non-Newtonian simulations have been obtained from Santra *et al.*'s study [59]. However, Al_2O_3 /water nanofluids up to 4% show Newtonian behavior as Putra *et al.* [60] state in their study on natural convection of nanofluids. Thus, non-Newtonian model shows the highest error rate.

3.3. Pressure Drop Simulations for Water Flow

Pressure drop performance of the current single-phase model has also been checked with analytical correlations. Water flow case has been simulated by using 93031 node size through a circular pipe which has length of 2.11 m and inner diameter of 10 mm at Re=500, 1000, 1500. Results can be seen in Table 3.4. Analytical correlations to determine pressure drop for fully developed laminar flow in a circular pipe is described as;

$$\Delta P = f \frac{X}{D} \frac{\rho V^2}{2} \quad (3.3)$$

where f is the friction factor and explained as;

$$f = \frac{64}{Re} \quad (3.4)$$

Table 3.4 shows that simulation results give 0.89%, 3.85% and 6.55% compared to analytical results at Reynolds 500, 1000 and 1500, respectively. Error rate increases with increasing Reynolds number, but it reaches maximum deviation of 6.55% which is acceptable.

Table 3.4. Error rates (%) of pressure drop simulations at different Reynolds numbers.

Reynolds Number	500	1000	1500
Analytical Pressure Drop (Pa)	34.06	68.06	102.13
Numerical Pressure Drop (Pa)	34.36	70.68	108.82
Error Rate (%)	0.89	3.85	6.55

4. RESULTS AND DISCUSSION

4.1. Heat Transfer Analysis

Forced convection of a Newtonian fluid under laminar flow condition has been simulated. Newtonian water flow case has been studied under constant heat flux boundary condition at various Reynolds numbers. Single-phase model has been applied and 93031 nodes have been used to simulate water flow through a pipe with 2110 mm length and 10 mm inner diameter. Results have been compared with Hojjat *et al.*'s experimental study [41] and the Shah equation [57].

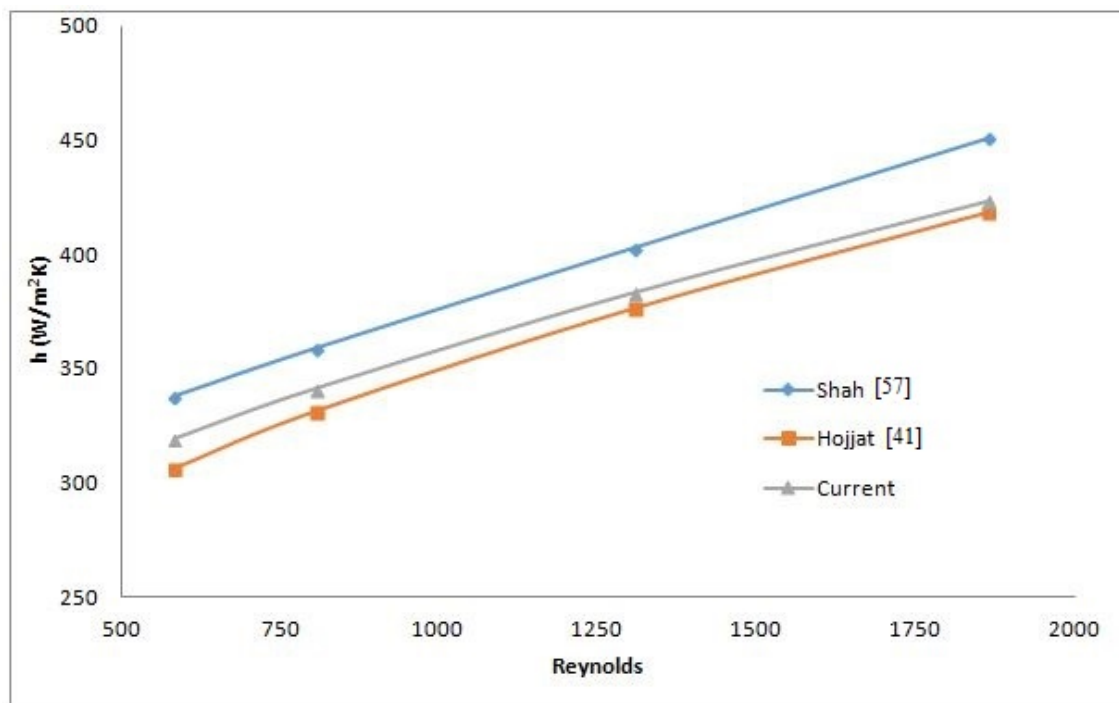


Figure 4.1. Convective Heat Transfer Coefficient Comparison of Water Flow at Various Reynolds Number.

As it can be seen in Figure 4.1, convective heat transfer coefficient increases with increasing Reynolds number and the same trend is observed among the Shah equation [57], Hojjat *et al.*'s experimental results [41] and the current numerical results. Results also revealed that numerical simulations have shown maximum deviation of 4.25% compared to experimental results [41] and error rate decreases as Reynolds

Table 4.1. Average convective heat transfer coefficient comparison for water flow.

Reynolds	Hojjat [41] (W/m^2K)	Current Numeric (W/m^2K)	Error(%)
584	306	319	4.25
806	331	341	3.02
1306	376	383	1.86
1862	418	423	1.20

number increases. These results can be seen in Table 4.1.

Secondly, forced convection of non-Newtonian 0.5% CMC/water based Al_2O_3 nanofluid with volume concentration up to 1.5% cases have been simulated and simulation results have been compared with Hojjat *et al.*'s experimental results [41]. CFD simulations have been done by applying Newtonian and non-Newtonian single-phase and two-phase models. Novel non-Newtonian two-phase modeling methods have been applied in this thesis. Mixture and Eulerian models have been utilized as non-Newtonian two-phase models. The same geometry and node number have been used as it was in the previous case.

Newtonian simulation results can be seen in Table 4.2 and results show that error rates of single and two-phase models increase as Peclet number and nanoparticle volume concentration increase. TP1 shows better agreement than TP2 models. Finally, we can conclude that TP1 Eulerian model shows the least average error rate of 7.90% compared to other single and two-phase models. Single-phase model gives higher error rates especially at high nanoparticle concentrations.

The same cases have been repeated by utilizing non-Newtonian models including single-phase and two-phase. When we compare Newtonian and non-Newtonian models, we can say that non-Newtonian models are better at all nanoparticle concentrations and Peclet numbers. Table 4.3 clearly shows that non-Newtonian TP1 Eulerian model gives the minimum average error rate among the other Newtonian and non-Newtonian models.

Table 4.2. Error rates (%) of Al_2O_3 -0.5% CMC/water experimental results and Newtonian single-phase and two-phase numerical models comparison.

ϕ_p	Pe	SP	TP1 Mixture	TP1 Eulerian	TP2 Mixture	TP2 Eulerian
0.10%	51200	5.71	5.58	3.11	6.18	4.38
	87600	7.53	6.49	3.76	9.02	6.09
0.20%	50400	5.85	6.15	4.94	8.25	6.03
	86600	6.85	8.18	5.88	10.36	7.06
0.50%	50000	8.72	9.20	7.36	10.85	9.11
	86400	7.98	9.31	8.11	11.13	10.12
1.00%	50400	11.17	10.11	9.48	12.21	11.10
	86400	11.42	9.58	9.29	13.30	12.05
1.50%	49634	15.62	14.16	13.37	14.94	13.02
	85200	16.33	14.36	13.67	14.60	13.58
Average Error (%)		9.72	9.31	7.90	11.08	9.25

Non-Newtonian single-phase model shows average error rate of 5.78% and it decreases with decreasing Reynolds number and nanoparticle concentration.

Furthermore, another non-Newtonian fluid flow case has been studied to examine non-Newtonian two-phase models. In this case, non-Newtonian characteristic of the nanofluid is caused by the high concentration of the nanoparticles. Chen *et al.*'s experimental study [37] has been repeated. 2.5% TNT/water nanofluid flow case has been simulated at 1700 Reynolds number by using 76508 nodes. Experimental setup has 3.97 mm diameter and 2 m length.

As it can be seen from Figure 4.2 and Table 4.4, single-phase Newtonian model shows better agreement with experimental results than that of two-phase Newtonian models.

Table 4.3. Error rates (%) of Al_2O_3 -0.5% CMC/water experimental results and non-Newtonian single-phase and two-phase numerical models comparison.

ϕ_p	Peclet	SP	TP1 Mixture	TP1 Eulerian	TP2 Mixture	TP2 Eulerian
0.10%	51200	0.17	0.10	0.15	1.21	1.34
	87600	0.71	0.71	0.68	2.06	2.09
0.20%	50400	1.22	1.48	1.13	2.36	1.38
	86600	3.12	3.09	2.68	3.20	3.05
0.50%	50000	4.82	4.81	2.81	5.01	4.16
	86400	4.59	4.50	3.62	6.27	4.11
1.00%	50400	8.61	8.60	6.37	8.65	6.69
	86400	10.22	10.05	8.80	10.52	9.85
1.50%	49634	11.97	11.95	10.25	12.82	12.12
	85200	12.40	12.37	11.36	13.07	12.61
Average Error(%)		5.78	5.77	4.79	6.52	5.74

Table 4.4. Error rates (%) of 2.5% TNT-water flow (Newtonian/non-Newtonian single-phase and two-phase models comparison).

X/D	SP Newt.	SP Non- Newt.	TP1 Mix. Newt.	TP1 Euler. Newt.	TP1 Mixt. Non-Newt.	TP1 Euler. Non-Newt.
50	19.66	0.68	22.38	22.78	1.64	2.15
100	13.73	5.66	14.84	15.34	4.58	3.85
150	13.01	6.04	13.58	14.28	5.40	4.47
200	17.81	1.63	18.16	19.01	1.21	0.07
250	9.20	8.36	9.42	10.33	8.09	6.86
300	0.20	15.80	0.06	0.90	15.63	14.30
350	7.16	9.09	7.28	8.47	8.95	7.50
400	3.14	12.04	3.22	4.51	11.94	10.35
450	0.21	14.46	0.14	8.29	14.37	12.72
Average Error(%)	9.35	8.20	9.90	11.55	7.98	6.92

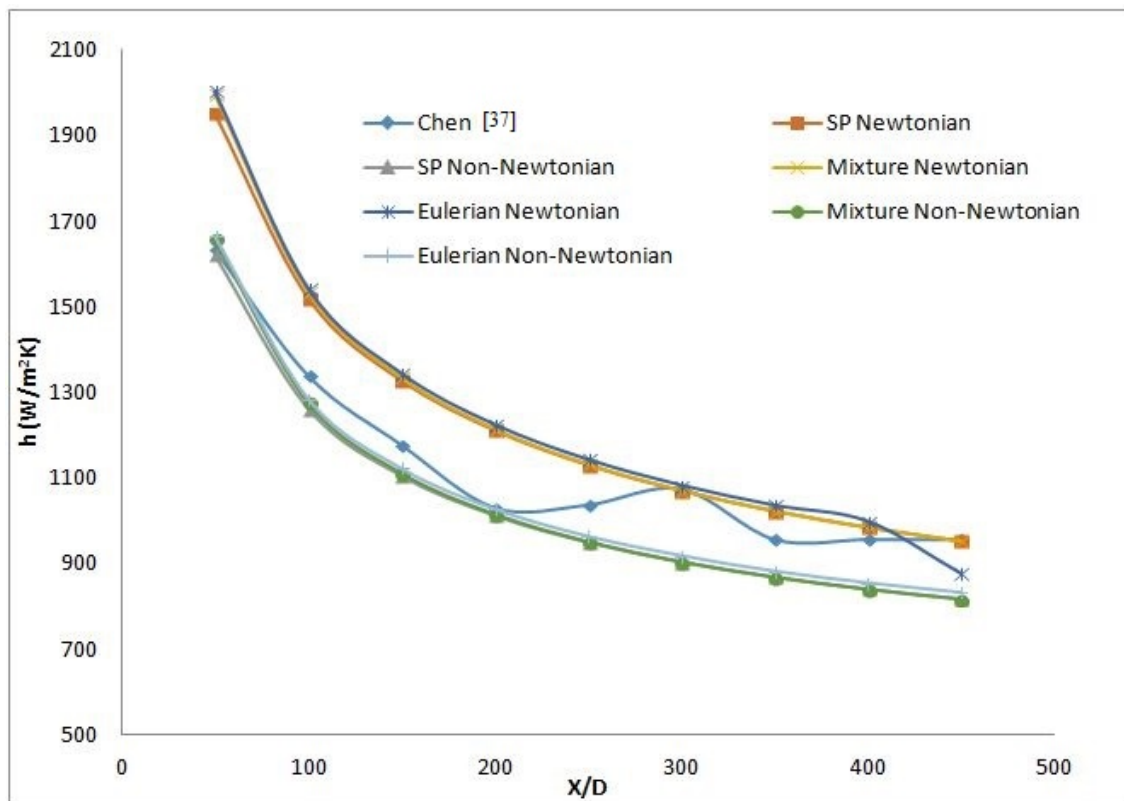


Figure 4.2. Convective Heat Transfer Coefficient Comparison of 2.5% TNT-Water Flow at $Re=1700$.

Among non-Newtonian models, TP1 Eulerian model gives the minimum average error rate. When we compare Newtonian and non-Newtonian models, it is obvious that non-Newtonian models are better than Newtonian models.

Overall heat transfer analysis results show that both TP1 and TP2 models are capable of simulating forced convection of nanofluids. Indeed, TP1 models gives more accurate results compared to TP2. However, one drawback of TP1 modeling method is that it requires more experimental data on rheological characteristics of nanofluids. This situation makes its application tougher than that of TP2 model. To apply TP2 method, rheological behavior of the base fluid must be experimentally determined and nanoparticle added rheology can be found by utilizing formulations that have been explained in the chapter 2. On the other hand, TP1 can be applied only if rheological behavior of nanofluid is experimentally known for all nanoparticle loading cases.

4.2. Pressure Drop Analysis

Pressure drop of non-Newtonian nanofluids is the other main concern of this study. Based on experimental results, Hojjat *et al.* [42] proposed a correlation to predict pressure drop of non-Newtonian nanofluids. Correlation can be seen as,

$$\frac{\Delta P}{\rho V^2} = \frac{1585}{Re} + 0.92 \quad (4.1)$$

In the current study, CFD results compared with their proposed correlation. Hojjat *et al.* [42] claim that the correlation can be used for different non-Newtonian nanofluids at various nanoparticle concentrations.

Non-Newtonian single-phase and two-phase models have been compared with the proposed model (Equation 4.1). Non-Newtonian Al_2O_3 -0.5 CMC/water flow through a pipe with 2110 mm length and 10 mm diameter case has been simulated by using 93031 nodes. Power law index and consistency index values have been obtained from Hojjat *et al.*'s experimental study [1].

Newtonian nanofluid flow comparison with the proposed model showed that correlation is not good at prediction of Newtonian nanofluid's pressure drop. As it can be seen from Table 4.5, error rates reach more than 200%. Results also show that increasing Reynolds number decreases the error rate and nanoparticle volume concentration does not have a strong effect on simulation results.

To check accuracy of Newtonian simulation and understand high error rates of non-Newtonian correlation and Newtonian simulation comparison, another pressure drop comparison has been done for Newtonian nanofluids. This time Equation 3.3 which is valid for Newtonian fluids compared with Newtonian nanofluid flow simulation results. Table 4.6 shows that all single and two-phase models give approximately the same results as it was found by Ambreen and Kim [29].

Table 4.5. Error rates (%) of Newtonian Al_2O_3 -water nanofluid pressure drop simulation comparison with proposed correlation for non-Newtonian nanofluids (Equation 4.1).

Concentration	Re	SP	TP1	TP1	TP2	TP2
			Mixture	Eulerian	Mixture	Eulerian
0.10%	500	241.81	224.94	224.94	241.56	253.30
	1000	191.20	178.40	179.80	192.00	201.20
	1500	155.56	144.44	144.44	156.06	164.14
0.50%	500	241.56	225.43	225.43	240.34	251.10
	1000	191.20	178.00	178.00	190.80	199.60
	1500	155.56	144.44	144.44	155.56	162.63
1.00%	500	241.32	225.18	225.18	239.12	249.14
	1000	191.20	178.00	178.00	189.60	198.00
	1500	155.56	144.44	144.44	154.04	161.11
1.50%	500	241.08	224.69	224.69	236.92	246.70
	1000	191.20	178.00	178.00	188.40	196.40
	1500	155.56	144.44	143.94	153.03	160.10

Furthermore, non-Newtonian nanofluid flow simulation results have been compared with Equation 4.1. As it can be seen from Table 4.7, error rates decreases with increasing Reynolds number and nanoparticle concentration. Single-phase non-Newtonian model shows the least deviation from correlation's results.

Results reveal that error rate decreases with increasing Reynolds number. This may be due to wide usage range of the proposed correlation. As a future work recommendation, experimental test condition can be limited in the laminar flow regime and the correlation should be revised according to these experimental results.

On the other hand, single-phase Non-Newtonian model showed the least error rate. Among the two-phase models, two-phase 1 modeling method is better than two-phase 2 modeling. There is a significant difference at lower Reynolds numbers for all

Table 4.6. Error rates (%) of Newtonian Al_2O_3 -water nanofluid pressure drop simulation comparison with the analytical correlation for Newtonian fluids (Equation 3.3).

Concentration	Re	SP	TP1 Mixture	TP1 Eulerian	TP2 Mixture	TP2 Eulerian
0.10%	500	4.83	4.77	4.74	7.36	7.28
	1000	4.59	4.52	4.49	7.35	7.21
	1500	4.35	4.29	4.26	7.15	7.12
0.50%	500	4.74	4.75	4.72	7.32	7.29
	1000	4.52	4.53	4.50	7.25	7.24
	1500	4.28	4.29	4.26	7.13	7.11
1.00%	500	1.44	1.43	1.40	2.29	2.26
	1000	3.02	3.04	3.07	4.27	4.23
	1500	7.56	7.57	7.61	8.45	8.39
1.50%	500	4.77	4.81	4.78	5.37	5.33
	1000	4.53	4.57	4.54	5.23	5.22
	1500	4.29	4.32	4.30	5.06	5.03

numerical models.

Table 4.7. Error rates (%) of non-Newtonian Al_2O_3 -0.5% CMC/water nanofluid pressure drop simulation comparison with the proposed correlation for non-Newtonian nanofluids (Equation 4.1).

Concentration	Re	SP	TP1 Mixture	TP1 Eulerian	TP2 Mixture	TP2 Eulerian
0.10%	500	34.72	34.72	34.96	40.59	40.83
	1000	18.00	18.00	18.40	32.80	33.20
	1500	6.57	6.57	6.57	20.71	20.71
0.50%	500	23.23	27.63	27.87	38.14	38.14
	1000	9.20	12.40	12.40	28.40	28.80
	1500	1.52	0.51	0.51	18.69	18.69
1.00%	500	24.45	27.87	28.12	38.39	38.39
	1000	10.00	12.40	12.40	29.20	29.60
	1500	1.01	1.01	1.01	19.19	19.19
1.50%	500	25.43	28.85	29.10	39.12	39.36
	1000	11.20	13.20	13.20	30.40	30.40
	1500	0.00	1.52	1.52	20.71	20.71

4.3. Thermal Performance Analysis

To evaluate thermal performance of non-Newtonian nanofluids, heat transfer coefficient and pressure drop increment tests have been conducted in scope of the current study. Pipe geometry consists of 2 m length and 10 mm diameter. According to mesh independency tests, 93031 node size has been utilized. First of all, heat transfer increment was measured. Al_2O_3 -0.5% CMC/water nanofluid flow case has been repeated by using non-Newtonian TP1 Eulerian model.

Heat transfer coefficient increment ratio of 0.5% CMC/water based Al_2O_3 nanofluid to base fluid can be seen in Figure 4.3. As it can be observed in Table 4.8, results reveal that heat transfer increment rate gets bigger at higher nanoparticle concentrations and

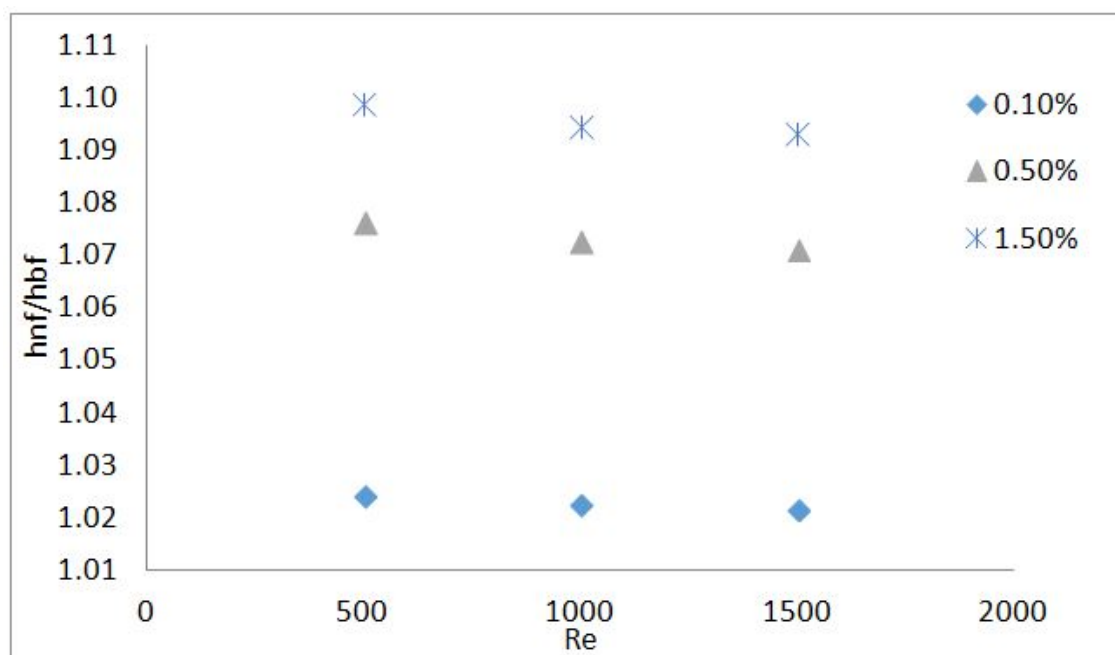


Figure 4.3. Heat Transfer Coefficient Increment Ratio of 0.5% CMC/Water Based Al_2O_3 Nanofluid to Base Fluid.

increasing Reynolds number slightly decreases the heat transfer increment rate. Similar results have also been observed by Minakov *et al.* [39], Hojjat *et al.* [41] and Javadpour *et al.* [47]. However, the heat transfer coefficient increases with increasing Reynolds number. Thus, rate of heat transfer increment can decrease with increasing Reynolds number even if the heat transfer coefficient increases with increasing Reynolds number. Maximum heat transfer coefficient increment ratio compared to base fluid is 9.88% at $Re=500$ and 1.5% nanoparticle concentration.

In scope of assessing heat transfer performance, pressure drop increment rate has also been checked. Al_2O_3 -0.5% CMC/water nanofluid flow case has been repeated by using non-Newtonian single-phase model at $Re=500$, 1000 and 1500.

Figure 4.4 and Table 4.9 clearly shows that increasing nanoparticle concentration increases pressure drop values. This situation causes more pumping power and less efficiency. On the other hand, increasing Reynolds number decreases the pressure drop increment rate. Therefore, we need to find the optimum point of heat transfer coefficient rate increment and pressure drop increment.

Table 4.8. Heat transfer coefficient increment rate (%) of 0.5% CMC/water based Al_2O_3 nanofluid.

Reynolds	0.1% Al_2O_3	0.5% Al_2O_3	1.5% Al_2O_3
500	2.42	7.64	9.88
1000	2.24	7.27	9.47
1500	2.15	7.10	9.32

Table 4.9. Pressure drop increment rate (%) of 0.5% CMC/water based Al_2O_3 nanofluid compared to base fluid.

Reynolds	0.1% Al_2O_3	0.5% Al_2O_3	1.5% Al_2O_3
500	3.78	24.11	30.96
1000	1.64	19.73	26.61
1500	0.49	17.28	24.25

Table 4.10 shows the ratio of convective heat transfer coefficient enhancement to pressure drop increase of non-Newtonian Al_2O_3 -0.5% CMC/water nanofluid flow. This table has been obtained from comparing data of Table 4.8 and Table 4.9. If the ratio is higher than 1, it means that heat transfer coefficient increment rate is higher than pressure drop increment rate.

Table 4.10 illustrates that it is more efficient to use non-Newtonian nanofluids at lower nanoparticle concentrations and higher Reynolds number. For instance, this ratio reaches its maximum of 1.02 at 0.1% nanoparticle concentration and 1500 Reynolds number.

Table 4.10. The ratio of convective heat transfer coefficient enhancement to pressure drop increase comparison of non-Newtonian Al_2O_3 -0.5% CMC/water nanofluid flow.

Nanofluid	Al_2O_3								
	0.10%			0.50%			1.50%		
Concentration									
Reynolds	500	1000	1500	500	1000	1500	500	1000	1500
$\frac{(h_{nf}/h_{bf})}{(\Delta P_{nf}/\Delta P_{bf})}$	0.99	1.01	1.02	0.87	0.90	0.91	0.84	0.86	0.88

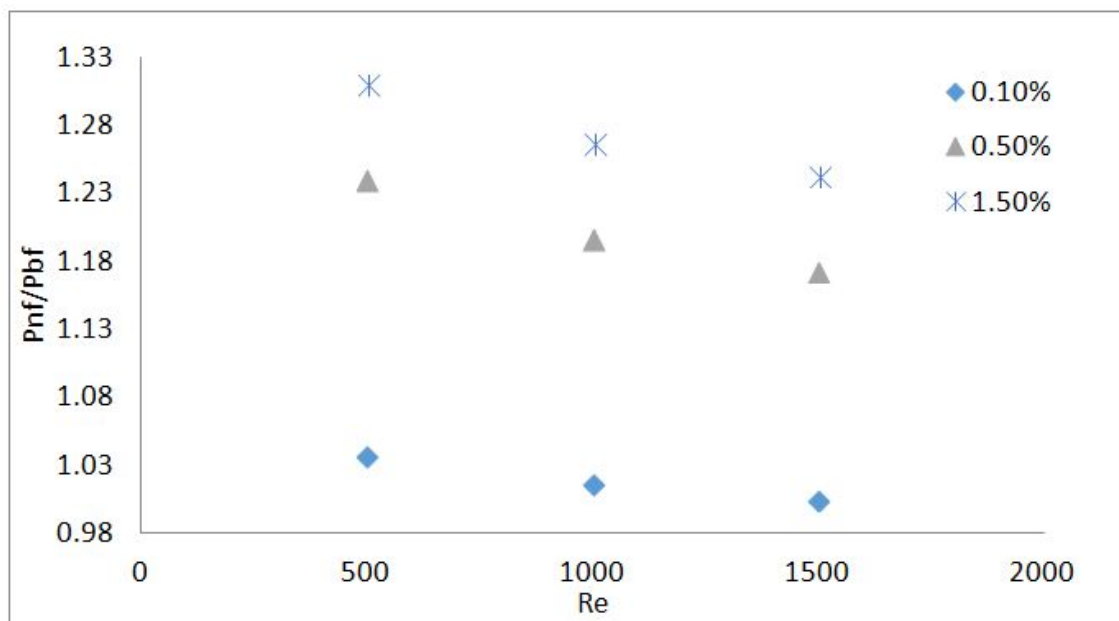


Figure 4.4. Pressure Drop Increment Ratio of 0.5% CMC/Water Based Al_2O_3 Nanofluid to Base Fluid.

Table 4.11. Heat transfer coefficient increment rate (%) of water based Al_2O_3 nanofluid compared to base fluid.

Reynolds	0.1% Al_2O_3	0.5% Al_2O_3	1.5% Al_2O_3
500	0.69	3.57	11.47
1000	0.95	4.84	15.16
1500	1.02	5.45	16.85

Finally, thermal performance of non-Newtonian nanofluids have been compared with that of Newtonian nanofluids. Water based Al_2O_3 nanofluid flow has been simulated to obtain Newtonian case under the same flow condition as it was in the non-Newtonian case.

As it can be seen in Figure 4.5 and Table 4.11, heat transfer increment rate increases as nanoparticle concentration and Reynolds number increases. It reaches maximum increment rate of 16.85% at 1.5% nanoparticle concentration and Reynolds number 1500.

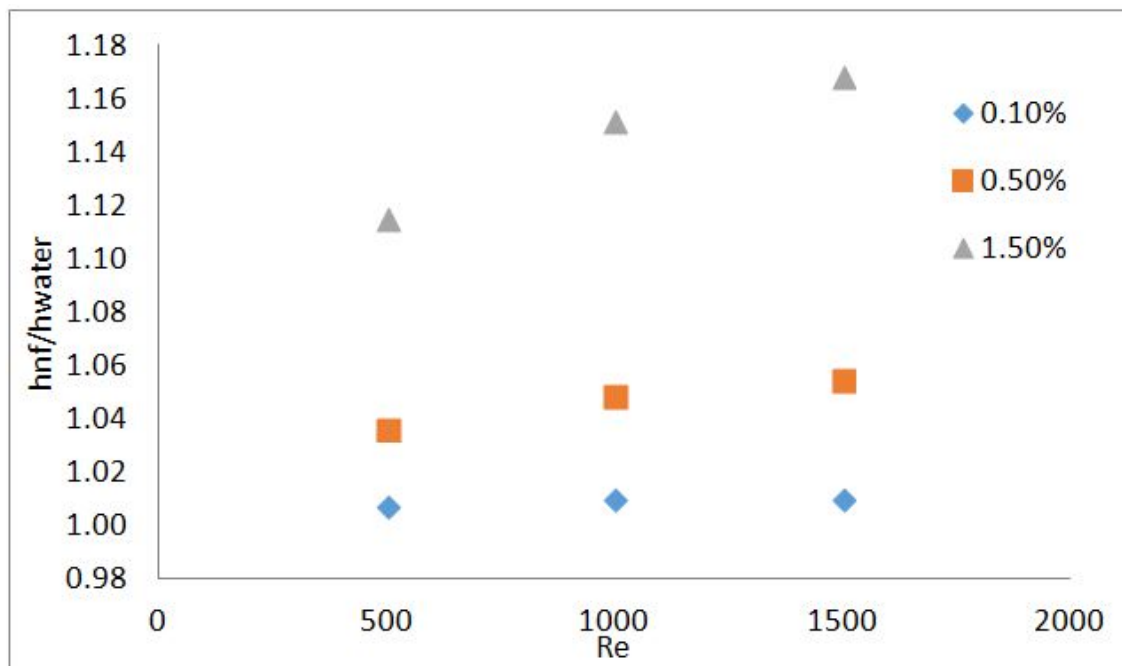


Figure 4.5. Heat Transfer Coefficient Increment Ratio of Water Based Al_2O_3 Nanofluid to Base Fluid.

Table 4.12. Pressure drop increment rate (%) of water based Al_2O_3 nanofluid compared to base fluid.

Reynolds	0.1% Al_2O_3	0.5% Al_2O_3	1.5% Al_2O_3
500	7.76	43.98	180.01
1000	7.84	43.99	179.77
1500	7.82	44.11	179.89

Pressure drop analysis shows that increasing nanoparticle concentration significantly increases the pressure drop and causes an inefficiency. In this case, more pumping power is needed. However, Reynolds number does not have a significant effect on pressure drop of Newtonian nanofluids. Figure 4.6 and Table 4.12 show that the pressure drop increment rate reaches 180.01% at 1.5% nanoparticle concentration and $Re=500$.

Table 4.13 shows the ratio of convective heat transfer coefficient enhancement to pressure drop increase of Newtonian Al_2O_3 -water nanofluid flow. This ratio is at its maximum at lower nanoparticle concentration and higher Reynolds number. However,

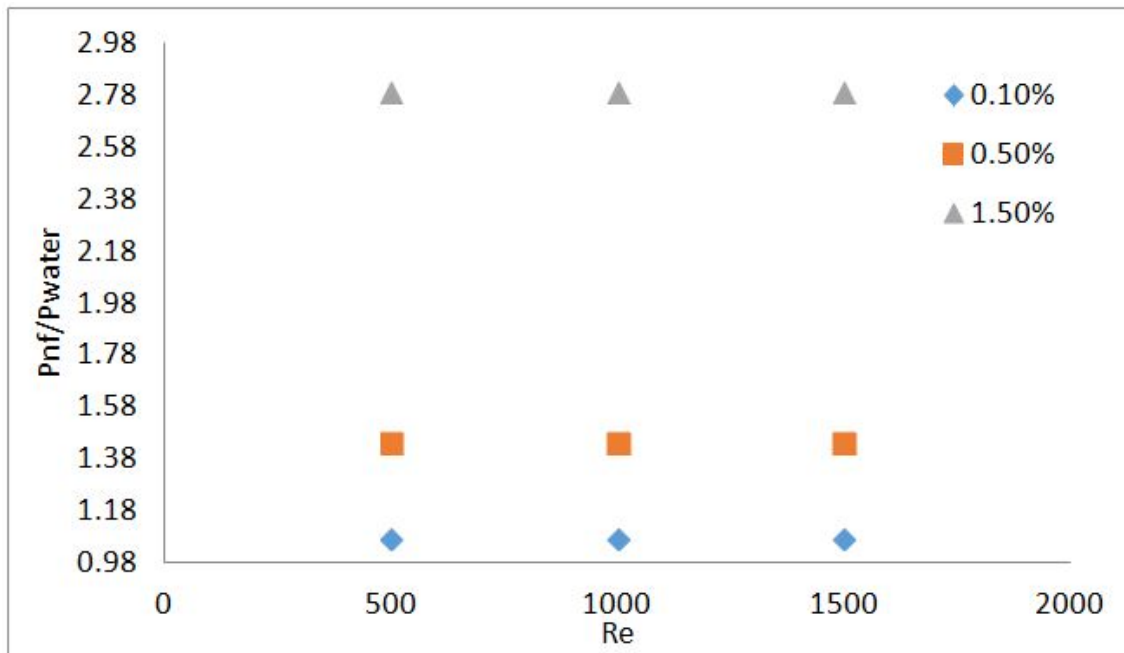


Figure 4.6. Pressure Drop Increment Ratio of Water Based Al_2O_3 Nanofluid to Base Fluid.

results reveal that using Newtonian nanofluid is not efficient. Heat transfer increment ratio is not higher than pressure drop for any concentration and at any Reynolds number. As Santra *et al.* [59] state in their study, more pumping power is needed for Newtonian fluids than non-Newtonian fluids. Tumuluri *et al.* [61] also show in their experimental study that shear thinning behavior causes a decrease in the pressure loss. Eventually, decreased pressure drop increases the thermal performance of the working fluid.

It can be concluded that Newtonian and non-Newtonian nanofluids show better thermal performance at lower nanoparticle concentration and higher Reynolds number as it was found by Purohit *et al.* [23].

Table 4.13. The ratio of convective heat transfer coefficient enhancement to pressure drop increase comparison of Newtonian Al_2O_3 -water nanofluid flow.

Nanofluid	Al_2O_3								
	0.10%			0.50%			1.50%		
Concentration									
Reynolds	500	1000	1500	500	1000	1500	500	1000	1500
$\frac{(h_{nf}/h_{bf})}{(\Delta P_{nf}/\Delta P_{bf})}$	0.93	0.94	0.94	0.72	0.73	0.73	0.40	0.41	0.42

5. CONCLUSION

In the current paper, non-Newtonian 0.5% CMC/water based Al_2O_3 nanofluid flow under laminar flow condition and constant wall heat flux boundary condition has been numerically studied in terms of heat transfer coefficient and pressure drop. Additionally, Newtonian water based 2.5% TNT nanofluid flow under laminar flow condition and constant wall heat flux boundary condition has been simulated. Finally, thermal performance analysis of Newtonian and non-Newtonian nanofluids has been investigated. These simulations have been conducted by using novel non-Newtonian two-phase models.

When we compare the proposed TP1 and TP2 methods, it needs to be kept in mind that base fluids change their rheological behavior after nanoparticle loading. TP1 and TP2 models have been proposed to define this changing rheology. As it was explained in the chapter 2, TP2 model does not require conducting experiments to evaluate viscosity of nanofluids for every nanoparticle concentration. To utilize TP2 model, viscosity of the base fluid needs to be measured experimentally. Nanoparticle added viscosity of nanofluid can be found by stated equations in the chapter 2. On the other hand, TP1 model requires experiments to evaluate nanofluid viscosity for every single nanoparticle loading case. In brief, TP2 method requires less experimental studies to find rheological behavior after nanoparticle loading.

Non-Newtonian 0.5% CMC/water based Al_2O_3 nanofluid flow is firstly investigated. Newtonian simulation results revealed that TP1 Eulerian model gives the minimum average error of 7.90%. Error rates increase with increasing Reynolds number and nanoparticle volume concentration. Non-Newtonian simulations show that TP1 Eulerian model is the best model because of the minimum deviation from the experimental results. It also can be said that non-Newtonian models are better than Newtonian models at all nanoparticle concentrations and Reynolds numbers at simulating non-Newtonian nanofluid flow.

2.5% TNT/water nanofluid is another non-Newtonian nanofluid case. In this case, nanofluid has its non-Newtonian characteristic because of high nanoparticle concentration. Among non-Newtonian models, TP1 Eulerian model gives the minimum average error rate. If Newtonian and non-Newtonian models are compared, it can be said that non-Newtonian models are better than Newtonian models.

Pressure drop analysis of non-Newtonian nanofluids showed that single-phase non-Newtonian model gives better results compared to non-Newtonian two-phase models and error rates decrease as Reynolds number increases. This may be due to wide usage range (laminar and turbulent) of the Hojjat *et al.*'s [42] proposed correlation. Additionally, it can be said that Hojjat *et al.*'s [42] proposed correlation cannot accurately predict the pressure drop of Newtonian fluids.

Pressure drop simulations of Newtonian nanofluids have also been compared with a correlation to predict pressure drop of Newtonian fluids. Results of this comparison showed that all Newtonian single-phase and two-phase models are good at predicting pressure drop of Newtonian fluids as it was also confirmed by Ambreen and Kim [29]. It is also shown that increasing nanoparticle concentration causes high pressure loss and inefficiency.

Heat transfer performance tests based on convective heat transfer increment and pressure drop increment rates showed that utilizing a shear thinning non-Newtonian nanofluid as a working fluid is more efficient than utilizing a Newtonian nanofluid. This is due to significant increase in pressure drop when we use a Newtonian nanofluid as it was stated at Santra *et al.*'s study [59]. It also should be known that shear thinning behavior causes lower pressure loss [61]. On the other hand, decreasing nanoparticle concentration and increasing Reynolds number increase thermal performance of both Newtonian and non-Newtonian nanofluids.

As a future work, a new correlation to predict the pressure drop of non-Newtonian nanofluids only in laminar flow regime should be proposed to give more accurate results. Additionally, two phase non-Newtonian models can be tested with many other

nanoparticle and base fluid combinations in turbulent flow and various boundary conditions. In terms of non-Newtonian nanofluids' thermal performance, numerical and experimental studies need to be conducted in turbulent flow regime.

Non-Newtonian nanofluids show promising heat transfer increment characteristics. Thus, they also need to be utilized as a working fluid of heat exchangers, air conditioning systems, nuclear reactors, radiators, etc. and their application should be investigated in terms of cost-effective aspect.

REFERENCES

1. Hojjat, M., S. G. Etemad, R. Bagheri and J. Thibault, “Rheological characteristics of non-Newtonian nanofluids: experimental investigation”, *International Communications in Heat and Mass Transfer*, Vol. 38, No. 2, pp. 144–148, 2011.
2. Maxwell, J. C., *A treatise on electricity and magnetism*, Vol. 1, Clarendon press, 1881.
3. Masuda, H., A. Ebata and K. Teramae, “Alteration of thermal conductivity and viscosity of liquid by dispersing ultra-fine particles. Dispersion of Al_2O_3 , SiO_2 and TiO_2 ultra-fine particles”, *Netsu Bussei*, 1993.
4. Choi, S. U. and J. A. Eastman, *Enhancing thermal conductivity of fluids with nanoparticles*, Tech. rep., Argonne National Lab., IL (United States), 1995.
5. Mukherjee, S. and S. Paria, “Preparation and stability of nanofluids-a review”, *IOSR Journal of Mechanical and civil engineering*, Vol. 9, No. 2, pp. 63–69, 2013.
6. Kakaç, S. and A. Pramuanjaroenkij, “Single-phase and two-phase treatments of convective heat transfer enhancement with nanofluids—a state-of-the-art review”, *International Journal of Thermal Sciences*, Vol. 100, pp. 75–97, 2016.
7. Vanaki, S. M., P. Ganesan and H. Mohammed, “Numerical study of convective heat transfer of nanofluids: a review”, *Renewable and Sustainable Energy Reviews*, Vol. 54, pp. 1212–1239, 2016.
8. Hamilton, R. L. and O. Crosser, “Thermal conductivity of heterogeneous two-component systems”, *Industrial & Engineering chemistry fundamentals*, Vol. 1, No. 3, pp. 187–191, 1962.
9. Heyhat, M., F. Kowsary, A. Rashidi, M. Momenpour and A. Amrollahi, “Ex-

- perimental investigation of laminar convective heat transfer and pressure drop of water-based Al_2O_3 nanofluids in fully developed flow regime”, *Experimental Thermal and Fluid Science*, Vol. 44, pp. 483–489, 2013.
10. Chon, C. H., K. D. Kihm, S. P. Lee and S. U. Choi, “Empirical correlation finding the role of temperature and particle size for nanofluid (Al_2O_3) thermal conductivity enhancement”, *Applied Physics Letters*, Vol. 87, No. 15, p. 153107, 2005.
 11. Kamali, R. and A. Binesh, “Numerical investigation of heat transfer enhancement using carbon nanotube-based non-Newtonian nanofluids”, *International Communications in Heat and Mass Transfer*, Vol. 37, No. 8, pp. 1153–1157, 2010.
 12. Maiga, S. E. B., C. T. Nguyen, N. Galanis and G. Roy, “Heat transfer behaviours of nanofluids in a uniformly heated tube”, *Superlattices and Microstructures*, Vol. 35, No. 3, pp. 543–557, 2004.
 13. Suresh, S., K. Venkitaraj, P. Selvakumar and M. Chandrasekar, “Effect of Al_2O_3 –Cu/water hybrid nanofluid in heat transfer”, *Experimental Thermal and Fluid Science*, Vol. 38, pp. 54–60, 2012.
 14. Wen, D. and Y. Ding, “Experimental investigation into convective heat transfer of nanofluids at the entrance region under laminar flow conditions”, *International journal of heat and mass transfer*, Vol. 47, No. 24, pp. 5181–5188, 2004.
 15. Akhavan-Zanjani, H., M. Saffar-Avval, M. Mansourkiaei, F. Sharif and M. Ahadi, “Experimental investigation of laminar forced convective heat transfer of Graphene–water nanofluid inside a circular tube”, *International Journal of Thermal Sciences*, Vol. 100, pp. 316–323, 2016.
 16. Yang, Y., Z. G. Zhang, E. A. Grulke, W. B. Anderson and G. Wu, “Heat transfer properties of nanoparticle-in-fluid dispersions (nanofluids) in laminar flow”, *International Journal of Heat and Mass Transfer*, Vol. 48, No. 6, pp. 1107–1116, 2005.

17. Cabaleiro, D., L. Colla, F. Agresti, L. Lugo and L. Fedele, “Transport properties and heat transfer coefficients of ZnO/(ethylene glycol+ water) nanofluids”, *International Journal of Heat and Mass Transfer*, Vol. 89, pp. 433–443, 2015.
18. Pourfayaz, F., N. Sanjarian, A. Kasaeian, F. R. Astarai, M. Sameti and S. Nasirivatan, “An experimental comparison of SiO_2 /water nanofluid heat transfer in square and circular cross-sectional channels”, *Journal of Thermal Analysis and Calorimetry*, Vol. 131, No. 2, pp. 1577–1586, 2018.
19. İlhan, B. and H. Ertürk, “Experimental characterization of laminar forced convection of hBN-water nanofluid in circular pipe”, *International Journal of Heat and Mass Transfer*, Vol. 111, pp. 500–507, 2017.
20. Noghrehabadi, A. and R. Pourrajab, “Experimental investigation of forced convective heat transfer enhancement of $\gamma-Al_2O_3$ /water nanofluid in a tube”, *Journal of Mechanical Science and Technology*, Vol. 30, No. 2, pp. 943–952, 2016.
21. Utomo, A. T., H. Poth, P. T. Robbins and A. W. Pacek, “Experimental and theoretical studies of thermal conductivity, viscosity and heat transfer coefficient of titania and alumina nanofluids”, *International Journal of Heat and Mass Transfer*, Vol. 55, No. 25-26, pp. 7772–7781, 2012.
22. Maiga, S. E. B., S. J. Palm, C. T. Nguyen, G. Roy and N. Galanis, “Heat transfer enhancement by using nanofluids in forced convection flows”, *International journal of heat and fluid flow*, Vol. 26, No. 4, pp. 530–546, 2005.
23. Purohit, N., V. A. Purohit and K. Purohit, “Assessment of nanofluids for laminar convective heat transfer: A numerical study”, *Engineering Science and Technology, an International Journal*, Vol. 19, No. 1, pp. 574–586, 2016.
24. Colla, L., L. Fedele and M. Buschmann, “Laminar mixed convection of TiO_2 -water nanofluid in horizontal uniformly heated pipe flow”, *International Journal of Thermal Sciences*, Vol. 97, pp. 26–40, 2015.

25. Elahmer, M., S. Abboudi and N. Boukadida, “Nanofluid effect on forced convective heat transfer inside a heated horizontal tube”, *International Journal of Heat and Technology*, Vol. 35, No. 4, pp. 874–882, 2017.
26. Ho, C., C. Chang, W.-M. Yan and P. Amani, “A combined numerical and experimental study on the forced convection of Al_2O_3 -water nanofluid in a circular tube”, *International Journal of Heat and Mass Transfer*, Vol. 120, pp. 66–75, 2018.
27. Göktepe, S., K. Atalık and H. Ertürk, “Comparison of single and two-phase models for nanofluid convection at the entrance of a uniformly heated tube”, *International Journal of Thermal Sciences*, Vol. 80, pp. 83–92, 2014.
28. Moghadassi, A., E. Ghomi and F. Parvizian, “A numerical study of water based Al_2O_3 and Al_2O_3 -Cu hybrid nanofluid effect on forced convective heat transfer”, *International Journal of Thermal Sciences*, Vol. 92, pp. 50–57, 2015.
29. Ambreen, T. and M.-H. Kim, “Comparative assessment of numerical models for nanofluids’ laminar forced convection in micro and mini channels”, *International Journal of Heat and Mass Transfer*, Vol. 115, pp. 513–523, 2017.
30. Sekrani, G. and S. Poncet, “Further investigation on laminar forced convection of nanofluid flows in a uniformly heated pipe using direct numerical simulations”, *Applied Sciences*, Vol. 6, No. 11, p. 332, 2016.
31. Behroyan, I., S. M. Vanaki, P. Ganesan and R. Saidur, “A comprehensive comparison of various CFD models for convective heat transfer of Al_2O_3 nanofluid inside a heated tube”, *International Communications in Heat and Mass Transfer*, Vol. 70, pp. 27–37, 2016.
32. Kole, M. and T. Dey, “Enhanced thermophysical properties of copper nanoparticles dispersed in gear oil”, *Applied Thermal Engineering*, Vol. 56, No. 1-2, pp. 45–53, 2013.

33. Chhabra, R. P. and J. F. Richardson, *Non-Newtonian flow and applied rheology: engineering applications*, Butterworth-Heinemann, 2011.
34. Phuoc, T. X. and M. Massoudi, “Experimental observations of the effects of shear rates and particle concentration on the viscosity of Fe_2O_3 -deionized water nanofluids”, *International Journal of Thermal Sciences*, Vol. 48, No. 7, pp. 1294–1301, 2009.
35. Kole, M. and T. Dey, “Effect of aggregation on the viscosity of copper oxide-gear oil nanofluids”, *International Journal of Thermal Sciences*, Vol. 50, No. 9, pp. 1741–1747, 2011.
36. Minakov, A. V., V. Y. Rudyak, D. Guzei and A. S. Lobasov, “Measurement of the heat transfer coefficient of a nanofluid based on water and copper oxide particles in a cylindrical channel”, *High Temperature*, Vol. 53, No. 2, pp. 246–253, 2015.
37. Chen, H., W. Yang, Y. He, Y. Ding, L. Zhang, C. Tan, A. A. Lapkin and D. V. Bavykin, “Heat transfer and flow behaviour of aqueous suspensions of titanate nanotubes (nanofluids)”, *Powder Technology*, Vol. 183, No. 1, pp. 63–72, 2008.
38. Paul, T. C., A. Morshed, E. B. Fox and J. A. Khan, “Thermal performance of Al_2O_3 nanoparticle enhanced ionic liquids (NEILs) for concentrated solar power (CSP) applications”, *International Journal of Heat and Mass Transfer*, Vol. 85, pp. 585–594, 2015.
39. Minakov, A., A. Lobasov, D. Guzei, M. Pryazhnikov and V. Y. Rudyak, “The experimental and theoretical study of laminar forced convection of nanofluids in the round channel”, *Applied Thermal Engineering*, Vol. 88, pp. 140–148, 2015.
40. He, Y., Y. Men, X. Liu, H. Lu, H. Chen and Y. Ding, “Study on forced convective heat transfer of non-Newtonian nanofluids”, *Journal of Thermal Science*, Vol. 18, No. 1, pp. 20–26, 2009.

41. Hojjat, M., S. G. Etemad and R. Bagheri, “Laminar heat transfer of non-Newtonian nanofluids in a circular tube”, *Korean Journal of Chemical Engineering*, Vol. 27, No. 5, pp. 1391–1396, 2010.
42. Hojjat, M., S. G. Etemad, R. Bagheri and J. Thibault, “Pressure drop of non-Newtonian nanofluids flowing through a horizontal circular tube”, *Journal of Dispersion Science and Technology*, Vol. 33, No. 7, pp. 1066–1070, 2012.
43. Hojjat, M., S. G. Etemad, R. Bagheri and J. Thibault, “Laminar convective heat transfer of non-Newtonian nanofluids with constant wall temperature”, *Heat and Mass Transfer*, Vol. 47, No. 2, pp. 203–209, 2011.
44. Garg, P., J. L. Alvarado, C. Marsh, T. A. Carlson, D. A. Kessler and K. Annamalai, “An experimental study on the effect of ultrasonication on viscosity and heat transfer performance of multi-wall carbon nanotube-based aqueous nanofluids”, *International Journal of Heat and Mass Transfer*, Vol. 52, No. 21-22, pp. 5090–5101, 2009.
45. Ding, Y., H. Alias, D. Wen and R. A. Williams, “Heat transfer of aqueous suspensions of carbon nanotubes (CNT nanofluids)”, *International Journal of Heat and Mass Transfer*, Vol. 49, No. 1-2, pp. 240–250, 2006.
46. Mahrood, M. R. K., S. G. Etemad and R. Bagheri, “Free convection heat transfer of non-Newtonian nanofluids under constant heat flux condition”, *International Communications in Heat and Mass Transfer*, Vol. 38, No. 10, pp. 1449–1454, 2011.
47. Javadpour, A., M. Najafi and K. Javaherdeh, “Experimental study of steady state laminar forced heat transfer of horizontal annulus tube with non-Newtonian nanofluid”, *Journal of Mechanical Science and Technology*, Vol. 31, No. 11, pp. 5539–5544, 2017.
48. Moraveji, M. K., S. M. H. Haddad and M. Darabi, “Modeling of forced convective heat transfer of a non-Newtonian nanofluid in the horizontal tube under constant

- heat flux with computational fluid dynamics”, *International Communications in Heat and Mass Transfer*, Vol. 39, No. 7, pp. 995–999, 2012.
49. Labib, M. N., M. J. Nine, H. Afrianto, H. Chung and H. Jeong, “Numerical investigation on effect of base fluids and hybrid nanofluid in forced convective heat transfer”, *International Journal of Thermal Sciences*, Vol. 71, pp. 163–171, 2013.
50. Xuan, Y. and W. Roetzel, “Conceptions for heat transfer correlation of nanofluids”, *International Journal of heat and Mass transfer*, Vol. 43, No. 19, pp. 3701–3707, 2000.
51. Pak, B. C. and Y. I. Cho, “Hydrodynamic and heat transfer study of dispersed fluids with submicron metallic oxide particles”, *Experimental Heat Transfer an International Journal*, Vol. 11, No. 2, pp. 151–170, 1998.
52. Miller, A. and D. Gidaspow, “Dense, vertical gas-solid flow in a pipe”, *AIChE journal*, Vol. 38, No. 11, pp. 1801–1815, 1992.
53. Kakaç, S. and A. Pramuanjaroenkij, “Analysis of convective heat transfer enhancement by nanofluids: single-phase and two-phase treatments”, *Journal of Engineering Physics and Thermophysics*, Vol. 89, No. 3, pp. 758–793, 2016.
54. Schiller, V., “A drag coefficient correlation”, *Z. Vereines Ingenieure*, Vol. 77, pp. 318–320, 1933.
55. Ranz, W., W. R. Marshall *et al.*, “Evaporation from drops”, *Chem. Eng. Prog.*, Vol. 48, No. 3, pp. 141–146, 1952.
56. Manninen, M., V. Taivassalo, S. Kallio *et al.*, “On the mixture model for multiphase flow”, Technical Research Centre of Finland, 1996.
57. Shah, R., “Thermal entry length solutions for the circular tube and parallel plates”, *Third National Heat Mass Transfer Conference, Indian Institute of Technology*,

- Bombay, India*, Vol. 1, pp. 11–75, 1975.
58. Velagapudi, V., K. R. Konijeti and K. S. C. Aduru, “Empirical correlations to predict thermophysical and heat transfer characteristics of nanofluids”, *Thermal Science*, Vol. 12, No. 2, pp. 27–37, 2008.
59. Santra, A. K., S. Sen and N. Chakraborty, “Study of heat transfer due to laminar flow of copper–water nanofluid through two isothermally heated parallel plates”, *International Journal of Thermal Sciences*, Vol. 48, No. 2, pp. 391–400, 2009.
60. Putra, N., W. Roetzel and S. K. Das, “Natural convection of nano-fluids”, *Heat and mass transfer*, Vol. 39, No. 8-9, pp. 775–784, 2003.
61. Tumuluri, K., J. L. Alvarado, H. Taherian and C. Marsh, “Thermal performance of a novel heat transfer fluid containing multiwalled carbon nanotubes and microencapsulated phase change materials”, *International journal of heat and mass transfer*, Vol. 54, No. 25-26, pp. 5554–5567, 2011.